

Published in final edited form as:

Sci Transl Med.; 12(548): . doi:10.1126/scitranslmed.aaz7715.

MHC class II invariant chain-adjuvanted viral vectored vaccines enhances T cell responses in humans

Ilaria Esposito^{#1,§}, Paola Cicconi^{#2}, Anna Morena D'Alise^{#3,‡}, Anthony Brown¹, Marialuisa Esposito³, Leo Swadling^{1,†}, Peter Johannes Holst^{4,8,12}, Maria Rosaria Bassi⁴, Mariano Stornaiuolo⁵, Federica Mori³, Ventzislav Vassilev⁶, Wenqin Li¹, Timothy Donnison¹, Chiara Gentile⁷, Bethany Turner¹, Annette von Delft¹, Mariarosaria Del Sorbo³, Federica Barra³, Alessandra Maria Contino³, Adele Abbate³, Ettore Novellino⁵, Allan Randrup Thomsen⁸, Jan Pravsgaard Christensen⁸, Armin Lahm³, Fabiana Grazioli³, Virginia Ammendola³, Loredana Siani³, Stefano Colloca³, Paul Klenerman^{1,2}, Alfredo Nicosia^{7,9,10}, Lucy Dorrell^{1,11}, Antonella Folgori^{3,*}, Stefania Capone^{3,*}, Eleanor Barnes^{1,2,*;±}, on behalf of the PEACHI Consortium

The PEACHI Consortium: In addition to PEACHI Consortium members who are authors Eleanor Barnes, Anthony Brown, Stefania Capone, Paola Cicconi, Lucy Dorrell, Ilaria Esposito, Marialuisa Esposito, Antonella Folgori, Federica Mori, Leo Swadling, Bethany Turner, Ventzislav Vassilev, Annette von Delft

the following PEACHI Consortium members are collaborators who have contributed to study design, data analysis and interpretation:

Carly Bliss¹, Emma Ghaffari¹, Felicity Hartnel¹¹, Jakub Kopycinski¹, Shokouh Makvandi-Nejad¹, Verity Nevin¹, Dorota Borys⁶, Dominique Boutriau⁶, Landry Cochard⁶, Lan Lin⁶, Frank Struyf⁶, Tomáš Hanke^{11,13}, Ciaran Bannan¹⁴, Colim Bergin¹⁴, Matthias Hoffman¹⁵, Patrick Schmid¹⁵, Pietro Vernazza¹⁵, Clair Gardiner¹⁶, Elena Woods¹⁶

*Corresponding author. E-mail: ellie.barnes@ndm.ox.ac.uk.

‡Present address: Nouscom Srl, 00128 Rome, Italy

§Present address: Centre for Experimental Medicine & Rheumatology, William Harvey Research Institute, E1 4NS London, U.K.

†Present address: Division of Infection & Immunity – UCL Rayne Institute, WC1E 6BT London, U.K

Author contributions: E.B., S. Capone, A.F., P.C., A.M.D., A.N., A.v.D., V.V., P.K., L.D. S. Colloca, P.J.H. designed the study/ protocols. I.E., P.C., A.M.D., S. Capone, A.B., M.E., W.L., C.G., T.D., M.D.S., F.B., A.M.C., M.S., A.L., F.G., V.A., L.S., P.K., E.B., A.F. performed the research and analysis. E.N., M.R.B., A.R.T., J.P.C. provided resources and funding. I.E., P.C., A.M.D., A.B., S. Capone, A.F., and E.B. wrote the manuscript. B.T. and F.M. led project management. E.B. was the principal investigator.

Competing interests: V.V. is an employee of GSK and owns restricted shares of the company. S.Colloca, A.F., A.N. and A.L. are named inventors on patent application [WO 2006133911 (A3)] submitted by Institute of Research of Molecular Biology P. Angeletti PSA (IRBM) that covers Hepatitis C virus nucleic acid vaccine. A.N., A.L., S.Colloca and Riccardo Cortese are inventors of patent application [WO 2003031588 (A2)] submitted by Institute of Research of Molecular Biology P. Angeletti PSA (IRBM) that covers Hepatitis C virus vaccine. S.Colloca, and A.N. are inventors on patent application [WO 2005071093 (A3)] submitted by Institute of Research of Molecular Biology P. Angeletti PSA (IRBM) that covers chimpanzee adenovirus vectors as carriers. M.R.B., A.M.D., A.F., P.J.H., A.N., Riccardo Cortese are inventors on patent application [2018/037045 (A1)] held by GlaxoSmithKline Biologicals SA and University of Copenhagen covering the fusion peptides with antigens linked to short fragments of Invariant chain (CD74). P.J.H., A.R.T. and J.P.C. are inventors on patent application [WO 2007062656 (A3)] submitted by University of Copenhagen detailing the use of MHC class II associated Invariant chain for virus vectored vaccines. P.J.H., A.R.T. and J.P.C. are inventors on patent [WO 2010057501 (A1)] submitted by University of Copenhagen that covers the Invariant chain vaccine strategy. The P.J.H., J.P.C. and A.R.T. are entitled to a fraction of any net income that may derive from the commercialization of this patent. P.K. has acted as a consultant to Tibotec and Pfizer on antiviral therapy. The other authors declare that they have no competing interests.

¹Nuffield Department of Medicine, University of Oxford, OX3 7BN Oxford, U.K ²The Jenner Institute Laboratories, Nuffield Department of Medicine, University of Oxford, OX3 7DQ Oxford, U.K ³ReiThera s.r.l., 00128 Rome, Italy ⁴Center for Medical Parasitology, University of Copenhagen, DK-2200 Copenhagen, Denmark ⁵Department of Pharmacy, University of Naples Federico II, 80131 Naples, Italy ⁶GSK Vaccines, 1330 Rixensart, Belgium ⁷Department of Molecular Medicine and Medical Biotechnology, University of Naples Federico II, 80131 Naples, Italy ⁸Department of Immunology and Microbiology, University of Copenhagen, DK-2200 Copenhagen, Denmark ⁹CEINGE-Biotecnologie Avanzate, via Gaetano Salvatore 486, 80145 Naples, Italy ¹⁰Keires AG, 4051 Basel, Switzerland ¹¹Oxford NIHR Biomedical Research Centre, OX3 9DU Headington, U.K ¹²InProTher ApS, BioInnovation Institute, 2200 Copenhagen, Denmark ¹³International Research Centre for Medical Sciences, Kumamoto University, 2-39-1 Kurokami Chuo-ku Kumamoto 860-855, Japan ¹⁴St James' Hospital, D08 NHY1, Dublin, Ireland ¹⁵Division of Infectious Diseases and Hospital Epidemiology, Kantonsspital St Gallen, 9007 St Gallen, Switzerland ¹⁶School of Biochemistry and Immunology, Trinity College, 152-160 Pearse Street, Dublin, Ireland

These authors contributed equally to this work.

Abstract

Strategies to enhance the induction of high magnitude T cell responses through vaccination are urgently needed. MHC class II associated invariant chain (Ii) plays a critical role in antigen presentation, forming MHC class II peptide complexes for the generation of CD4⁺ T cell responses. Pre-clinical studies evaluating the fusion of Ii to antigens encoded in vector delivery systems have shown that this strategy may enhance T cell immune responses to the encoded antigen. We now assess this strategy in humans, using chimpanzee adenovirus 3 (ChAd3) and modified vaccinia Ankara vectors (MVA) encoding human Ii fused to the non-structural antigens (NS) of hepatitis C virus (HCV) in a heterologous prime/boost regimen. Vaccination was well tolerated and enhanced the peak magnitude, breadth, and proliferative capacity of anti-HCV T cell responses compared to non-Ii vaccines in humans. Very high frequencies of HCV-specific T cells were elicited in humans. Polyfunctional HCV specific CD8⁺ and CD4⁺ responses were induced with up to 30% of CD3⁺CD8⁺ cells targeting single HCV epitopes; these were mostly effector memory cells with a high proportion expressing T cell activation and cytolytic markers. No volunteers developed anti Ii T cell or antibody responses. Using a mouse model and in vitro experiments, we show that Ii fused to NS increases HCV immune responses through enhanced ubiquitination and proteasomal degradation. This strategy could be used to develop more potent HCV vaccines that may contribute to the HCV elimination targets, and paves the way for developing class-II Ii vaccines against cancer and other infections.

Introduction

Strategies to enhance the induction of high magnitude immune responses for the prevention and treatment of both infectious disease and cancer are urgently needed. In this study we evaluate the inclusion of full-length MHC class II associated invariant chain (Ii), also known as CD74, as a molecular adjuvant in viral vectored vaccines. The aim is to enhance anti-viral

T cell immune responses in humans and to understand the mechanism by which Ii enhances the potency of viral vectored immune responses.

Ii is a non-polymorphic type II transmembrane protein with multiple functional domains, highly conserved across mammalian species and widely expressed in different immune cell types. Ii is known to play a critical role in MHC class II antigen presentation, stabilising MHC class II α and β chains in the rough endoplasmic reticulum and directing exogenous antigen from endocytic compartments to the MHC II molecules (1). Efficient loading of antigen on MHC class II and presentation at the cell surface is required for the generation of effective CD4⁺ T cell responses. In efforts to enhance vaccine induced T cell immune responses, murine (mIi) and human (hIi) Ii sequences have been fused to transgenes encoded in a range of constructs including Adenoviral (Ad) vectors (2, 3), DNA plasmids (4), lentiviral vectors (5) and modified vaccinia Ankara (MVA) vectors (6) and assessed in pre-clinical small animal models and non-human primates (NHP) (7, 8). These studies have consistently shown that Ii increases both the magnitude and breadth of T cell responses to the transgene. Unexpectedly, an enhancement not only on CD4⁺ T cell induction, but also on the CD8⁺ T cell subset, associated with enhanced protection in both tumor and infectious disease models has been demonstrated in animals (9–11).

In order to develop Ii for use in humans, we determined the capacity of Ii to enhance Hepatitis C Virus (HCV)-specific T cell responses in ChAd and MVA viral vectors. We have previously developed replicative-defective chimpanzee adenoviral vectors (ChAd) (12); these have a clear advantage in that that pre-existing anti-vector immunity, which may limit vaccine efficacy in humans, is rarely encountered (13). Combining ChAd with MVA in heterologous prime/boost regimens has been shown to be effective in inducing high magnitude T cell responses against encoded immunogens in human studies, and this strategy is currently being assessed to develop vaccines against a range of infections including HIV (14), HCV (15), malaria (16), influenza (17) and tuberculosis (18), all infections where enhanced T cell immunity has been associated with viral control in natural history studies. In addition, following the recent paradigm shift in cancer therapy, with the development of therapeutic checkpoint inhibitors that restores T cell immunity leading to cancer cure in some patients (19), these vectors are in development as immunotherapy for prostate, bowel, cervical and other cancers (20). Whilst viral vectors generate robust cellular immune responses, further enhancing these with adjuvants, such as Ii, may be required for challenging diseases including cancer and chronic infections where T cells induction must overcome functional exhaustion and genetically diverse pathogens such as HCV and HIV where rapid T cell induction by vaccines may limit viral escape.

HCV was selected for the developmental pipeline since there remains a pressing need to develop an HCV vaccine, with an estimated 1.7 million new infections each year, commonly leading to persistent HCV viremia, liver cirrhosis and hepatocellular cancer (21). Recent data suggests that the World Health Organization targets for HCV elimination will not be met (22) without incorporating a prophylactic vaccine into therapeutic treatment strategies. Even a low-moderately effective vaccine would have a major beneficial impact on the elimination agenda (22–25). Whilst the correlates of protection for HCV immunity are not precisely defined, multiple lines of evidence suggest that HCV specific T cell immunity

plays a critical role in viral control (26–30) and therefore strategies to enhance anti-viral T cell responses are likely to improve vaccine efficacy. We therefore developed human and mouse Ii chain vaccines fused to an HCV genotype 1b non-structural (NS) antigen and showed that anti-viral T cell responses (especially for CD8+ T) generated by Ii fused vaccines, were enhanced, accelerated and sustained cells in mice and non-human primates (31).

Here we report the safety profile and in-depth immune analysis where a viral vectored candidate vaccine for HCV fused to full length human invariant chain was administered to healthy volunteers of a phase I clinical trial. We also used experimental systems to investigate the mechanism of action behind the invariant chain adjuvant effect and determine the minimal domain required for the adjuvant effect.

Results

ChAd3-hliNSmut and MVA-hliNSmut vaccinations are well tolerated

Twenty-six subjects were screened for eligibility and 17 participants were recruited into a dose escalation study. Six subjects were enrolled in group 1 and received a low dose of the vaccine (ChAd3-hliNSmut 5×10^9 vp and MVA-hliNSmut 5×10^7 pfu) and eleven subjects were enrolled in group 2 and received a standard dose of the vaccine (ChAd3-hliNSmut 2.5×10^{10} vp and MVA-hliNSmut 2×10^8 pfu). Comparisons of adverse events and immune responses are made with volunteers (n=19) vaccinated with non-Ii (but otherwise identical HCV vaccines) in previous studies (15, 32) (fig. S1 and table S1). We excluded subjects with autoimmune disease, a strong family history of autoimmune disease, and HLA B27 subjects, since anti-CD74 Abs have been detected in patients with HLA B27 associated ankylosing spondylitis (table S2) (33–35). The median age at first vaccination was 44 years (IQR 23–53), 47% were female and participants were predominantly (82%) Caucasian.

Overall, both ChAd3-hliNSmut and MVA-hliNSmut were very well tolerated. There were no suspected unexpected serious adverse reactions (SUSARs) or related serious adverse events (SAEs). The most frequently reported AEs were those typically seen in response to viral vectored vaccines including pain at the injection site, headache, fatigue, myalgia, and feverishness. A total of 116 solicited local and systemic adverse events were reported: 21 after priming vaccinations (8 in Group 1 and 13 in Group 2) and 95 after boosting vaccinations (24 in Group 1 and 71 in Group 2). The majority (83%) of AEs were mild or moderate and resolved within 72 hours. ChAd3-hliNSmut vectored vaccine was less reactogenic (3/21, 14.2% grade 2 and no grade 3) than MVA-hliNSmut vectored vaccine (43/95, 45% grade 2 and 18/95, 18% grade 3). Twenty grade 3 AEs followed boosting vaccinations (5/24, 21% in Group 1 and 15/71, 21% in Group 2); these included muscle ache, general discomfort, fatigue, feverishness, joint ache, headache, nausea and pain at the injection site. The proportion of volunteers reporting moderate or severe solicited AEs and the nature of the AEs following ChAd3-hliNSmut (2/17, 11.7%) and MVA-hliNSmut (12/15, 80%) was not significantly different from that observed following the same dose of ChAd3-NSmut (1/9, 11.1%) and MVA-NSmut (6/8, 75%) without invariant chain (Fig. 1A–F). Unsolicited adverse events with Ii vectored vaccines that were reported included

gastrointestinal symptoms, flu-like syndrome, fatigue and cough. These were also generally mild in nature as listed in table S3. None of the participants withdrew due to AEs.

A transient reduction in total lymphocyte count was observed within 24 hours of administration of MVA-hIiNSmut in most volunteers (fig. S2); eight episodes were classified as grade 2 ($0.5-0.8 \times 10^9$ cells/L) and one was grade 3 ($0.2-0.5 \times 10^9$ cells/L). Mean (standard deviation, SD) counts ($\times 10^9$ cells/L) at day 56 and day 57 were 2.06 (0.3) and 0.99 (0.4) for volunteers in Group 1 ($P=0.02$), and 1.31 (0.5) and 0.77 (0.4) in Group 2 ($P<0.0001$), respectively. These changes were not associated with any symptoms and lymphocyte counts returned to normal by day 84 in all cases. There were no other grade 3 or systematic laboratory abnormalities detected (table S4).

Inclusion of hIi sequence in vaccine improves magnitude, breadth, and durability of HCV-specific T cell responses

We evaluated if the inclusion of Ii influenced the magnitude of the T cell response induced by the vaccination. All volunteers responded to ChAd3-hIiNSmut vaccination with a peak post-prime response at d14 or d28 post vaccination (Group 1: median, 366; range 60-1717 spot-forming cells (SFCs)/ 10^6 peripheral blood mononuclear cells (PBMCs); fig. S3A, Group 2: median, 1850; range, 417-7168 SFCs/ 10^6 PBMCs; Fig. 2A). T cell responses were significantly boosted by MVA-hIiNSmut peaking at d63 post vaccination (Group 1: prime vs boost $P=0.017$, group 2 prime vs boost $P=0.0011$) (Group 1: median, 2173; range 520-10210 SFCs/ 10^6 PBMCs; fig. S3A, Group 2: median, 6253; range, 2130-12577 SFCs/ 10^6 PBMCs; Fig. 2A) that was still elevated until d238 (Group 1: median, 903; range 193-3362 SFCs/ 10^6 PBMCs; fig. S3A, Group 2: median, 1662; range, 238-3113 SFCs/ 10^6 PBMCs; Fig. 2A).

When compared to T cell responses induced in healthy volunteers by the ChAd3NSmut and MVA-NSmut vaccines given at same dose, Ii inclusion significantly increased the magnitude of T cell responses at most time points after prime and boost (Fig. 2B Group 2, peak responses: d14: with Ii; median, 1852; range, 1115-7168 versus without Ii; median, 465; range, 0-3905 SFCs/ 10^6 PBMCs; $P<0.0001$; d63: with Ii; median, 6252; range, 213-12577 versus without Ii; median, 3108; range 1173-9513 $P=0.0067$).

The response in volunteers vaccinated with ChAd3/MVA-hIiNSmut vaccine was maintained at the end of study (EOS) although there was not statistical significance between groups. An assessment of total magnitude of the T cell response to vaccination over time by Area Under the Curve (AUC) analysis (Fig. 2C) revealed significantly higher values for volunteers receiving hIiNSmut compared to non-Ii NSmut (without Ii; median, 31254; range, 10777-89295 versus with Ii; median, 73758; range, 27226-154862; $P=0.001$).

Administration of Ii-including vaccines at low dose resulted in equivalent T cell responses to those induced by non-Ii vaccines given at a 4-5 fold higher dose. (Group 1, fig. S3B).

T cell responses at peak post boost were broad and targeted five to six peptide pools covering the HCV NS antigen in most volunteers, independently of the HLA haplotype (Fig. 2D).

A broader response in terms of number of targeted HCV NS peptide pools was seen in individuals receiving hliNSmut vaccines compared to those receiving non-Ii NSmut constructs, especially at peak post-prime and at d98 (Fig. 2E; post prime $P=0.007$; d98 $P=0.008$). The hierarchy of antigen recognition was similar in the two vaccine cohorts with NS3 protease and helicase regions (NS3p and NS3h) eliciting the most dominant responses; these were significantly increased by the inclusion of Ii in the vaccine constructs (day 63, peak response after MVA boost, Fig. 2F; NSp: with Ii; median, 1783; range, 635-2695 versus without Ii; median, 445; range, 130-1203; $P<0.0001$; NSh: with Ii; median, 2770; range, 170-4000 versus without Ii; median, 1310; range, 605-3330; $P=0.023$).

In a subset of volunteers, the cross-reactivity of the T cell responses at d63 was assessed by stimulation of PBMCs using an HCV genotype 3a peptide set in parallel to the 1b peptide set. The inclusion of hIi to NS antigen had no effect on the degree of inter genotypic cross-reactivity (fig. S4).

Immune response to hli and to ChAd3 vector

To monitor if vaccination generated an immune response against the hIi vaccine component, T cell and antibody responses against hIi were assessed at baseline, peak post-ChAd3 prime (d28), MVA boost (d63) and at end of study (EOS). No positive T cell responses were detected for Ii antigens in IFN- γ ELISpot assays (Fig. 3A and table S5). One individual from Group 2 (018) repeatedly had detectable T cell responses to Ii, but these always coincided with a high background of T cell responses in the assay, and so failed to meet established criteria for a positive response (>48 SFC/ 10^6 PBMCs and a response to HCV antigens $>3\times$ background). Volunteers 016 and 025 showed weak antibody recognition of CD74 antigen at baseline, but no volunteers showed an increase in CD74 antibody recognition following vaccination (Fig. 3B).

Low titers of ChAd3 cross-neutralization activity (range 21-197) were detected at baseline in serum of 11 volunteers, similarly distributed in groups 1 and 2. The remaining 6 volunteers had titers below the detection limit of the assay. ChAd3 neutralizing titers increased in most volunteers upon ChAd3-hIiNSmut prime by 4 weeks post-vaccination (fig. S5A). Interestingly, two volunteers did not seroconvert after vaccination and were amongst the top responders to ChAd3-hIiNSmut prime vaccination. There was no significant correlation between ChAd3 nAb at baseline and T cell response to ChAd3-hIiNSmut neither post ChAd3 prime nor post MVA boost (fig. S5B).

MVA-hIiNSmut boost induces polyfunctional CD4+ and CD8+ T cell subsets with enhanced and sustained proliferative capacity

We next evaluated frequencies and functionality of vaccine-induced CD4+ and CD8+ T cell subsets using fresh PBMCs from group 2 volunteers (using intracellular cytokine [ICS] assays), at peak magnitude post-boost (d63) and at the EOS. The CD8+ T cell response dominated compared to CD4+ T cell responses, with a high proportion of cells producing IFN- γ (up to 20% for CD8+ and 3% for CD4+ T cells) followed by TNF- α and IL-2 at boost that were largely sustained until the EOS (Fig. 4A-C). CD154 (CD40 ligand), which is upregulated on activated CD4+ T cells, was highly expressed as was the degranulation

marker CD107a in CD8+ T cell populations (Fig. 4D). Simplified Presentation of Incredibly Complex Evaluation (SPICE) analysis showed that vaccine-induced HCV-specific CD4+ and CD8+ T cells were polyfunctional and composed of a mixed population of single, dual and triple cytokine producers in approximately equal proportions after boost vaccination and at EOS (fig. S6). In keeping with the IFN- γ ELISpot data, antigen-specific T cell frequencies induced by hIiNSmut (compared to non-Ii NSmut at peak magnitude post-MVA boost), revealed significantly higher percentages of IFN- γ and TNF- α positive HCV NS-specific CD8+ (IFN- γ P=0.01; TNF- α P=0.01) and CD4+ (IFN- γ P=0.01; TNF- α P=0.005), as well as a larger proportion of CD8+ secreting IL2 (P=0.006) in volunteers receiving hIiNSmut vaccines (fig. S7).

We evaluated whether the fusion of Ii to NS could also have an impact on the long-term proliferative capacity of vaccine-induced memory T cells. For this we stimulated EOS PBMC from each volunteer, using the two HCV NS peptide pools (named pools 1 and 2) to which the subject generated the highest responses, and one pool (pool 3) to which a weaker, though still positive response was detected according to IFN- γ ELISpot data at peak post-MVA boost. Robust proliferative responses could be detected to all antigens tested. Importantly, the proliferative capacity of both CD4+ and CD8+ T cells was clearly increased in volunteers receiving hIiNSmut vaccines compared to the non-Ii vaccines, with statistically significant differences shown for the CD8+ T cell populations (Fig. 5A–B and fig. S8 pool 1: P=0.04; pool 2: P=0.004; pool 3: P=0.004).

Phenotyping of CD8+ HLA class I pentamer+ HCV-specific vaccine-induced T cells

To evaluate if Ii fusion to encoded antigens may impact not only magnitude but phenotype and functional characteristics of antigen specific CD8+ T cells we used HLA class I pentamers in HLA-matched volunteers (table S6–S7). We tracked the percentage of pentamer+ CD8+ cells in volunteers receiving hIi vaccines over time and detected remarkable frequencies (up to 20%) against a single epitope (Fig 6A-B). Phenotypic analysis revealed that CD38 and PD1 were highly expressed at peak post-ChAd3 prime and peak post-MVA boost at similar frequencies to volunteers that received non-Ii vaccines. These declined by the EOS, though the expression of PD1 remained higher in volunteers vaccinated with Ii vaccines (Fig. 6C). HLA-DR expression was found to be significantly lower with Ii vaccines at peak post-prime (P=0.044) and peak post-boost(P=0.029), though not at the EOS (Fig.6C). Granzyme A was also highly expressed and maintained through the EOS. CD127, a marker of long-lived memory T cells, increased from vaccination to EOS phase in a similar fashion in volunteers receiving Ii-including and non-Ii vaccines (Fig. 6C and fig. S9).

Memory T cell subpopulations were determined through the assessment of surface markers CCR7 and CD45RA on pentamer+ cells. All populations including effector memory T cells (Tem CD45RA-CCR7-), central memory (Tcm CD45RA-CCR7+), “terminally differentiated” effector memory T cells (TemRA CD45RA+ CCR7-) and naïve-like memory (Tn CD45RA+ CCR7+) could be detected. However, linkage to Ii increased the proportion of the effector memory populations measured especially at peak post prime and peak post boost compared to non-Ii vaccines (Fig. 6D). Granzyme B, Tbet, and Eomes expression did

not change over time. For both vaccinated groups (fig. S9 and fig. S10A–B) Tbet⁺/Eomes⁺ expression, which defines CD8⁺ populations with cytolytic and memory functions, were found at high frequency throughout, whilst Tbet⁻/Eomes⁺ populations (defining exhausted populations) were found only at low frequency (fig. S10C).

Phenotyping of CD4⁺ HLA class II tetramer⁺ HCV-specific vaccine-induced T cells

Phenotypic analysis was carried out using HLA class II tetramers to identify and characterize CD4⁺ T cells targeting epitopes in the NS region known to be immune dominant in natural HCV infection (table S6–S7) (36–38). High frequencies of HCV-specific CD4⁺ T cells could be detected in volunteers receiving Ii-including vaccine, especially at peak post-MVA boost (Fig. 7A–B). Similar to CD8⁺ populations, CD127 expression was more highly expressed in IiNSmut vaccines at peak time points following vaccination, increasing towards the EOS to reach similar frequencies in the two vaccine cohorts (Fig. 7C). CD28, a well-characterized T cell costimulatory receptor, was highly expressed by more than 90% of HCV-specific CD4⁺ at all time points tested with no major differences between Ii and non-Ii vaccines (fig. S11A–B). Using CCR7 and CD45RA staining we observed that effector memory CD4⁺ populations dominated at peak responses and were higher compared to non-Ii vaccines, but a more balanced distribution of memory responses was seen at the EOS. Similar to effects seen in CD8⁺ T cells, the inclusion of Ii as adjuvant increased the proportion of effector memory-like CD4⁺ T cells at peak after prime and at peak after boost compared to non-Ii vaccines (Fig. 7D). In spite of the high number of HCV specific CD4⁺ T cells generated, no volunteers developed antibodies to HCV by the EOS, as assessed using a standard clinical assay.

Ii enhances CD8⁺ T cell responses by promoting antigen K48-linked ubiquitination and degradation

Having demonstrated an adjuvant effect of full length Ii in humans we aimed to map the Ii minimal functional domain and to understand the mechanism of action. For this, we generated Ad5 vectors encoding full length (FL) murine Ii (mIi) and also variants with deleted domains, fused to the model antigen ovalbumin (OVA) (Fig. 8A). As expected, mice vaccinated with Ad5-mIi-OVA showed enhanced OVA-specific IFN- γ -secreting CD8⁺ T cell responses compared to Ad5-OVA (Fig. 8B, $P < 0.0001$). Adjuvant activity was fully retained in deletion mutants lacking trimerization (mIi1-105) ($P = 0.042$), CLIP (mIi1-80) ($P < 0.0001$), KEY domains (mIi1-75) ($P = 0.002$), and the endosomal sorting signal (ESS) (mIiD-17) ($P < 0.0001$). Although mIi1-75 retained the adjuvant effect, a shorter mutant (mIi1-50) containing only the N-terminal endolysosomal sorting signal plus most of the trans-membrane domain was ineffective at enhancing immune responses (Fig. 8B, $P = 0.991$). We therefore show that domains essential for the Ii physiological role in antigen presentation are fully dispensable for the enhancement of CD8⁺ T cell responses, whereas amino acids 50-75 are essential for T cell enhancement.

Consistent with the *in vivo* data, the immunostimulatory mIi1-75 fragment was able to increase the presentation of OVA peptide SIINFEKL via H-2Kb on CD11c⁺ bone marrow-derived dendritic cells upon Ad5 infection ($P = 0.033$), whereas the mIi1-50 variant was ineffective (Fig. 8C). This effect was proteasomal dependent, given the complete loss of the

Ii-mediated enhancement of antigen presentation in cells treated with the proteasome inhibitor MG132 (Fig. 8C). Inhibition of antigen degradation in endocytic vesicles by Pepstatin A/E64, inhibitors of lysosomal proteases, had no effect (Fig. 8C).

The canonical pathway for proteasome-mediated degradation of antigen utilizes polyubiquitin chains formed on target antigens via ubiquitin Lys48 (K48) residue. We therefore assessed antigen ubiquitination using mIi-OVA mutants by immunoprecipitation of ubiquitinated proteins from total cell lysates. K48-mediated polyubiquitination was found only for mIi-OVA and mIi1-75, but not for the mIi1-50 fragment (Fig. 8D), suggesting that ubiquitin linkage is involved in the degradative fate imparted by mIi on fused antigens. Using a mIi1-75 variant with mutation of the single lysine residue at position 63, we demonstrated that Ii itself is not the target of a specific E3 ligase but acts as a degron signal to facilitate ubiquitination of the fused antigen (fig. S12A–C).

We hypothesized that the amino acids between residues 50 and 75 of mIi may be sufficient to promote ubiquitination and enhance CD8⁺ T cell responses. We generated an Ad5 encoding OVA fused to polypeptide 55-75 (YQQQGRLDKLTITSQNLQLES), a short unstructured region of Ii devoid of the transmembrane domain (Fig. 8E). Vaccination of mice with mIi55-75 OVA resulted in enhanced OVA-specific CD8⁺ T cell responses, similarly to full length mIi (Fig. 8F, mIi55-75 vs OVA $P=0.015$; mIi vs OVA $P=0.01$; consistently fusion with mIi55-75 promotes poly-ubiquitination of OVA (Fig. 8G). Finally, ubiquitination and increased proteasomal degradation was also demonstrated for hIi-fused HCV NSmut antigen, supporting this as the mechanism responsible for enhancing CD8⁺ T cell responses in the human study (Fig. 8H).

Discussion

We show that a viral vectored vaccine encoding an immunogen fused to human Ii and delivered in a prime/boost regimen significantly enhances CD4⁺ and CD8⁺ T cells against the encoded immunogen in humans. The inclusion of human Ii enhanced the magnitude of the T cell response to the encoded immunogen 4-fold at peak following ChAd3 prime and 2-3-fold after MVA boost, and these responses were largely maintained to the end of the study. The breadth (number of HCV antigenic pools) of the immune response against the encoded immunogen was also significantly enhanced by the inclusion of Ii chain; generating a broad immune response is likely to be particularly important in vaccines that seek to protect against genetically variable pathogens such as HCV and HIV. Our data also suggest that inclusion of Ii is promising in terms of dose sparing, since the same immune response was achieved with lower dose of vaccine; this may be of relevance for difficult to produce vectors, for mass vaccination campaigns or in vulnerable populations where a lower vaccine dose may be desirable.

The inclusion of invariant chain did not affect the tolerability of ChAd3 and MVA vectored vaccines that appeared safe, with an adverse event profile that is typical for viral vectored vaccine studies. There were no related serious adverse events, and the majority of events were mild. A transient fall in lymphocyte count was observed but quickly recovered without any clinical consequences. Transient lymphopenia is a well-recognized effect of both viral

infections and also interferon therapy. Most likely this represents migration to secondary lymphoid tissues and we have previously observed this effect using non-Ii viral vectored vaccines in association with the regulation of genes involved in lymphocyte trafficking and activation (32).

We show that Ii vaccines delivered in heterologous prime/boost generated high magnitude, polyfunctional CD4+ and CD8+ T cell responses that were dominated by IFN- γ production, followed by TNF- α and IL-2, similar to that observed in pre-clinical studies in mice and non-human primates (8). CD8+ T cell responses were particularly enhanced with more than 10% of total CD8+ T cells targeting the immunogen in many volunteers after boost vaccination. Using HLA class I and class II multimers we were able to characterize in detail the CD8+ and CD4+ T cells induced by vaccination. We show that in some cases up to 30% CD8+ and 0.13% of CD4+ T cells target single epitopes. As expected, CD8+ and CD4+ T cells were highly activated at peak responses after prime and boost vaccination but not at the EOS, whilst high proportions of granzyme A and granzyme B required for effector functions were maintained to the EOS. We found that the proportion of effector CD4+ and CD8+ memory T cells were increased using Ii compared to non-Ii vaccines at all time points. This is relevant since Tem and TemRA subsets have been associated with protection against HIV, influenza and malaria in vaccine studies(39–41). Tbet and Eomes expression also indicated that a CD8+ T cell population with memory and cytolytic phenotypes were generated, whilst CD127 expression in CD8+ and CD4+ T cells increased over time, suggesting that vaccination induced a population of long-lived memory T cells. In keeping with this, we observed that Ii vaccine-induced T cells had a higher proliferative capacity at the EOS compared to non-Ii vaccines.

We assessed the impact of ChAd3 neutralizing antibody titers at baseline and after vaccination on T cell responses to the encoded transgene. Approximately two thirds of volunteers had low anti-ChAd3 antibody titers at baseline and these increased in all but 2 volunteers after vaccination. Although there was no overall correlation with the induction of immune responses after vaccination, these 2 volunteers had notably high T cell responses to the vaccine antigen after vaccination. Assessment of this correlation is limited by small numbers in this phase I study and larger cohorts are required to solidly establish the effects of low titer ChAd3 antibodies on immune induction.

In preclinical studies of Ii adjuvanted viral vector vaccines, T cell and antibody responses to autologous Ii were closely monitored with no evidence of immune responses elicited against homologous Ii (7, 8). However, recent studies have identified IgG antibodies targeting the CLIP region of CD74 (Ii) as a potential biomarker for ankylosing spondylarthritis (AS), detected in up to 85% of patients with AS compared to 6-8% of control subjects (33–35). In this study we therefore carefully monitored for the breaking of tolerance to hIi using two complimentary assays that can detect anti-Ii T cell and Ab responses. We also elected to exclude volunteers with HLA-B27 which is strongly associated with AS (42) and also volunteers with a history, or strong family history, of autoimmune disease. We found no evidence that either antibodies or T cells were generated against Ii at any of the multiple time points assessed. Since tolerance to Ii was preserved in this study, and since there is no

evidence that the presence of anti-CD74 Abs are implicated in AS pathogenesis, future studies using Ii may not need to exclude HLA-B27 subjects.

We found in mice that that Ii modulates CD8+ T cell immune responses by triggering fused antigens for K48-specific ubiquitination, proteasome-mediated degradation and increased presentation by MHC class I. It is very unlikely that the machinery of the classical MHC class II presentation pathway is involved in the enhanced T cell responses to Ii-linked antigens as Ii retains this effect when CLIP, KEY or trafficking domains are removed or when the MHC class II pathway is blocked by neutralization of endosomes or inhibitors of lysosomal proteases. Using a number of Ii deletion mutants to map the minimal functional domain and to gain insights into the mode of action, we found that a short Ii peptide derived from an unstructured and not-well characterized region of the protein is sufficient to recapitulate Ii-mediated ubiquitination, increased MHC class I antigen presentation and *in vivo* adjuvant activity in mice. The effects of this minimal peptide sequence for use as a genetic adjuvant now requires evaluation in human studies.

In a recent pre-clinical study, human Ii was systematically truncated to determine the minimal length of the protein needed for its adjuvant activity when fused to a malaria antigen encoded by an adenovirus vaccine (9). These investigators demonstrated that a minimal fragment of 26 amino acids consisting of the transmembrane domain of human Ii was sufficient to increase a T cell response in mice, and that antigen stabilization by multimerization mediated by the transmembrane domain led to Ii mediated immune enhancement. However, the minimal region identified in the malaria study differs from the minimal region that we have identified and the proposed mechanism of action of Ii in the two studies is also different. Together these data suggest that Ii chain fragments may enhance T cell responses through multiple pathways that may be antigen-dependent, due to differences in immunogenicity, folding, stability and the presence of structural domains or sorting signals of different antigens linked to invariant chain.

Limitations of this study include the fact that this is a small phase I study. Whilst the number of volunteers is appropriate for a first in man study, the results may not be directly transferable to cohorts with different demographics and will require replication. In particular we excluded volunteers who were HLA B27; since we found no evidence of immune responses against Ii, future studies could include this subject subset. Furthermore, the enhancing effect of Ii may not universally apply to all immunogens and will require validation in human studies using vaccines encoding different immunogens. Whilst we have identified a minimal length of Ii required to give the adjuvant effect *in vitro* and in pre-clinical models, this will require validation in human studies.

HCV exists as seven major genotypes that are genetically divergent and prevalent in different geographical regions(43). The NSmut vaccine antigen corresponds to HCV genotype 1b (44) and has previously been shown to generate T cells that show some cross reactivity to non-gt1b antigen (12); however, the inclusion of Ii did not significantly enhance the cross-reactivity of T cell responses to non-gt1b HCV antigens and we recommend that consideration should be given to the design of new immunogens to target multiple HCV genotypes.

Finally, whilst we show that the inclusion of full length Ii in viral vectored vaccines may safely enhance high magnitude, polyfunctional T cell responses, larger studies with longer follow up may be required to assess the durability of this effect. The durability of immune responses is clearly an important criterion, required for effective prophylactic vaccine strategies. However, maximising and maintaining T cell induction for several months, as we have shown in this study, may be particularly useful for therapeutic vaccination strategies against chronic infection and cancer where new strategies to optimise disease control or cure are urgently needed.

Materials and Methods

Study Design

In this open-label study (ClinicalTrials.gov; NCT03688061), subjects were enrolled sequentially into two groups: group 1 (n=5) received ChAd3-hIiNSmut (5×10^9 viral particles, vp) and MVA-hIiNSmut (5×10^7 pfu) at day 0 and 56 respectively; group 2 (n=10) received ChAd3-hIiNSmut (2.5×10^{10} vp) and MVA-hIiNSmut (2×10^8 pfu), at the same intervals. Both groups of healthy volunteers vaccinated with ChAd3/MVA-hIiNSmut vaccines were compared to ChAd3/MVA-NSmut vaccines (Peachi 04, NCT02362271 (15) and HCV003 NCT01296451 (32)) (table S1). There was no blinding or randomization. For Ethics and Regulatory approval see Supplementary Materials. Primary data are reported in data file S1.

Participants—Healthy male and female volunteers aged 18-65 were included following informed consent. Exclusion criteria included pregnancy, personal history of autoimmune disease, history of major autoimmune disease in first degree relative, HLA type B27 positive at screening (table S2). All vaccinations/ study visits were performed at Oxford, UK. Approvals for the study were granted by the UK National Research Ethics Service, (NRES Committee London Harrow 16/LO/1539) and the UK Medicines and Healthcare Products Regulatory Agency (Eudract no. 2016-000983-41). The study was registered with ClinicalTrials.gov (NCT03688061). GCP compliance was independently monitored by the University of Oxford Clinical Trials and Research Governance office. A multinational independent data safety monitoring committee (DSMC) provided safety oversight. The study was conducted in accordance with the principles of the Declaration of Helsinki and good clinical practice (GCP).

Assessment of primary endpoints: safety and reactogenicity—Volunteers were observed for 30 minutes following immunization (60 minutes if first participant in each group). A safety review of the first three volunteers in each group was conducted by the Data and Safety Monitoring Committee (DSMC) 48 hours following each vaccination, before proceeding to further vaccinations. Both solicited and unsolicited AEs were collected. Study visits for safety evaluation occurred on vaccination days (D0 and D56), with a further 9 visits up to day 238 (EOS). Safety data included specific solicited symptoms collected by diary card during day 0-6 post each vaccination. Blood sample for evaluation of biochemical and/or hematological parameters were taken at days 0, 1, and 28 after each vaccination. HCV serology and viral quantification in blood were taken at the end of the trial.

Assessment of secondary endpoints: T cell responses—The cellular immune response was assessed in each subject after ChAd3-hIiNSmut and MVA-hIiNSmut prime-boost vaccination at low and standard dose. The induction of T cell responses to HCV epitopes was evaluated through IFN- γ ELISpot, Intracellular cytokine staining (ICS), HLA class I and class II multimer staining and cellular proliferation assays. Invariant chain specific T cells and antibody responses were evaluated.

Mechanistic studies—The mechanism of action and the mapping of the minimum functional domain of Invariant chain was assessed in cell-based assays and in mice. Adenovectors encoding for variants of murine Ii (mIi) deleted of well-known Ii domains fused to chicken ovalbumin model antigen (OVA) were generated. These mIi deleted variants were tested by measuring their effect on enhancement of antigen-specific immune response in vaccinated mice, on antigen presentation of OVA on MHC-I and antigen ubiquitination through western blot and immunoprecipitation assays.

Adenoviral and MVA constructs

ChAd3 and MVA vectors encoded the NS3–5 (1985 amino acids) of genotype 1b BK strain (accession number M58335) with the human Ii sequence (p35, NCBI reference sequence: NM_004355.2) inserted at the N-terminus of the NS transgene as previously described. A mutated form of NS5 gene was obtained by replacing the Gly-Asp-Asp sequence corresponding to amino acid positions 1711-1713 of the complete polyprotein with Ala-Ala-Gly. The mutations of these three residues inhibits or abolishes the potential replicative capacity of immunogen (NSmut antigen) (8). ChAd3-hIiNSmut was manufactured at Aeras (now IDT Biologika corporation) and fill-finished at Advent s.r.l. MVA-hIiNSmut was manufactured at IDT Biologika GmbH. Vaccine vials were stored at -80°C and thawed 30 minutes prior to administration. All vaccinations were given into the deltoid muscle. Ad5 vectors encoding full length and short variants of mIi fused to ovalbumin were generated as previously described (2). Further truncations of Ii were made by PCR. All Ad constructs were E1E3-deleted. Full length and truncated Ii sequences were cloned at the N-terminus of the transgene under HCMV and SV40pA. Gene synthesis was provided by GeneArt (Life Technologies).

HCV peptides and antigens

494 peptides of 15 amino acids, overlapping by 11 amino acids corresponding to the HCV NS immunogen were used in six pools (named F, G, H, I, L, and M) corresponding respectively to NS3p, NS3h, NS4, NS5A, NS5B I, NS5 BII. 53 peptides of 15 amino acids overlapping by 11 amino acids corresponding to full length of human CD74 p35 were utilized as pool. Peptides were used at $3\mu\text{g/ml}$ or $1\mu\text{g/ml}$ for use in ELISpot and ICS respectively. Peptide pools derived from HCV genotype 3a (GenBank accession D28917) were prepared identically.

Human IFN- γ ELISpot assays

IFN- γ ELISpot assays were performed directly ex vivo on freshly isolated PBMCs as described previously and in supplementary methods, using at 2×10^5 PBMCs per well, plated in triplicate (12, 15).

Intracellular cytokine staining (ICS)

ICS was performed as previously described and with better details in supplementary methods (12, 15). Antibodies used are listed in table S8. Analysis uses Flow Jo (TreeStar, LLC). Analysis of polyfunctionality was performed using Pestle and SPICE version 5.3, downloaded from <http://exon.niaid.nih.gov> (45).

MHC class II tetramer staining

PE-labelled, MHC class II tetramers were donated from the NIH Core Tetramer Facility (Atlanta, GA, USA). A total of 8 tetramers were used in the study (table S6). HLA-class II typing was performed for each subject (table S7). Thawed PBMC ($6-8 \times 10^6$ cells) were stained with Live dead-NIR and then stained with single or a combination of different tetramers (depending on HLA type of the single volunteer) for 60 minutes at 37°C (1µg/100µl) in 100 µl of RPMI medium (Sigma) with 10% human serum (Sigma), 1% of Penicillin-Streptavidin (GibcoBRL) and 2mM of L-Glutamine (GibcoBRL) (hR10 medium). After washing, cells were stained with surface antibodies listed in table S8 for 30 minutes in PBS at room temperature shielded from the light. A positive tetramer response was defined as a discrete cluster of cells and >0.004% tetramer+ CD4+ T cells and 3x baseline (pre-vaccination). This cut off was determined after an analysis of tetramer+ CD4+ cells in unimmunized individuals. Data were collected with BD FACS DIVA software and analysed with Treestar Flow Jo software (FlowJo, LLC). CD45RA/CCR7 subsets were analysed using Pestle and SPICE (45).

MHC class I pentamer staining

PE-labelled pentamers (Proimmune) comprising HLA-A*0201-bound HCV NS3₁₄₀₆₋₁₄₁₅ (KLSALGINAV) and HLA-A*0101-bound NS3₁₄₃₅₋₁₄₄₃ (ATDALMTGY) were used to stain HCV NSmut-specific CD8+ T cells, as previously described and in supplementary methods (12, 15). The specificity of pentamers was confirmed on HLA-matched pre-vaccination samples from healthy volunteers. Intracellular and intranuclear antibodies used are (listed in table S8). All FACS data were analysed by a custom-build LSR II flow cytometer (BD Biosciences). FACS and SPICE analysis was performed as for MHC class II tetramers.

Cellular proliferation assays

Ex vivo proliferation assay was performed on previously frozen isolated PBMC at the EOS. At day 0 2.5 µM cell trace violet reagent (CTV) was added to 1ml of aliquots of lymphocytes in PBS with immediate vortexing to ensure rapid and homogenous labelling of cells. Cells were incubated at room temperature for 10 minutes in the dark, then washed 3 times with RPMI (Sigma) supplemented with 10% human serum (hR10). CTV-labelled lymphocytes ($1-2 \times 10^6$ cells) were cultured in non-conditioned hR10 media and NS antigen (4µg/ml) and phytohemagglutinin (PHA) or DMSO (controls) for 5 days without any addition of cytokine. For each subject we selected the two HCV antigen pools (pools 1 and 2) that generated the highest responses and one pool (pool 3) that generated weaker, but still positive responses pre-defined using the IFN-γ ELISpot assay. Cells were harvested, stained

with surface antibodies, acquired through BD FACS DIVA software and analysed with Treestar Flow Jo software (FlowJo, LLC).

ELISA to detect anti-CD74 antibodies

Coating of Polystyrene 96-well plates (Thermo Scientific,) was performed with 150ng/well of human CD74 p35 ectodomain (hCD74(p35)ECD GSK, Belgium) in NaHCO₃ 50 mM pH 9.6 buffer incubated overnight at 4°C. Plates were washed, and blocked with 5% non-fat dry milk/0.05% Tween20 in PBS 1X (milk buffer) for 1 hour at 37°C. Human sera diluted 1:20 in milk buffer were tested in triplicate and incubated 2 hours at 25°C. Positive controls (Rabbit polyclonal anti-human CD74 immunogen Affipure, AbCam) were added (range 3ng/ml to 100 ng/ml). Naïve, human sera diluted 1:20 was used as the negative control. Secondary antibody (Monoclonal HRP conjugate mouse a-human IgG cross reactive with NHP and rabbit IgG, Invitrogen) diluted 1:500 in milk buffer was added and incubated for 1 hours at 25°C. After wash, plates were developed with TMB (3,3',5,5'-tetramethylbenzidine, Sigma) and reaction blocked with HCl 1N. Plates were read at 450/630 nm with an EnSight Multimode Plate Reader (PerkinElmer). Statistical analysis in set up experiments with sera from healthy donors (i.e. assessment of normality, appropriate data transformation and identification of statistical outliers) suggested a floating cut-point approach (46). A normalization factor has been calculated (0.061) during set up, to be added to each plate's negative control OD to determine the plate-specific cut-point.

Cell line cultures and infections

HeLa cells (ATCC) were cultured in Dulbecco's Modified Essential Medium (DMEM) (GibcoBRL) supplemented with 10% heat-inactivated Fetal Bovine Serum (FBS) (Hyclone) and 2mM L-glutamine (GibcoBRL) (R10 medium) at 37°C in a 5% CO₂/95% air atmosphere. Bone Marrow Dendritic Cells (BMDC) were obtained from femurs of 6-10-week-old female CB6F1 mice, a hybrid mouse strain obtained by a cross between female BALB/c and male C57BL6 mice and cultured in R10 with 10 ng/ml of recombinant murine granulocyte-macrophage colony-stimulating factor (rGM-CSF; Invitrogen) for 10 days. HeLa and BMDC cells were infected with adenoviral vectors at 50 MOI/cell and 200 MOI/cell respectively.

The following inhibitors (Sigma) were used: MG132 10µM, pepstatin (1µM)/ E64D (10µM) (ratio 1:1), chloroquine (500nM).

Immunoprecipitation Assay

HeLa cells were transfected with 2µg FLAG-Ubiquitin plasmid (Invitrogen) for 16 hours with Lipofectamine 2000 (Invitrogen). After transfection, cells were infected with viral vectors, treated with MG132 and lysed using lysis buffer (Tris-HCl pH 7.5 20mM, NaCl 150mM, EDTA pH 8 1mM, Triton 10% and protease inhibitors in PBS). Protein lysates were immunoprecipitated with anti-Ub-Lys48 antibody (10 µg clone Apu2 rabbit monoclonal, Millipore) for 16 hours at 4°C, followed by incubation with protein A sepharose CL-4B (500 µg GE Healthcare) for 45 minutes at 4°C. Immunocomplexes were eluted with 0.2% SDS in 75mM sodium phosphate buffer pH 7.5, boiled (95°C for 5 minutes), reduced with DTT (100 mM) and analyzed by Western blot. Expression of OVA

was detected using an anti-HA tag HRP-conjugated (Miltenyi Biotec, mouse monoclonal) at 1:5000. Expression of HCV transgene was detected using an anti-HCV NS3 (mouse monoclonal, Abcam) at 1:1000. For detection, peroxidase-conjugated anti-mouse antibody (Sigma) at 1:5000 was used. Signals were visualized using ECL SuperSignal West Pico Chemiluminescent substrate (Thermo Scientific).

Animals and vaccination

All experimental procedures were approved by the local animal ethics council and were performed in accordance with national and international laws and policies (UE Directive 2010/63/UE; Italian Legislative Decree 26/2014). The ethical committee of the Italian Ministry of Health approved this research. Six-week-old female C57 mice were purchased from Charles River (Como, Italy). Viral vectors were administered via intramuscular injection in the quadriceps (50 μ l per side) at 3×10^6 vp. For the short variant and mutated forms of mLi the dose of injection was 1×10^6 vp.

Antigen presentation assay

Presentation of ovalbumin-derived peptide SIINFEKL was performed as previously described (47). Briefly, upon Adenovirus infection, BMDC were harvested, washed in RPMI twice, and resuspended in PBS. The expression of CD11c and H2-Kb-SIINFEKL complexes on live cells was quantitated by fluorescence-activated cell sorter using CD11c-Pecy7 (BD Biosciences) and 25-D1.16 antibodies (Biolegend).

Statistical analysis

GraphPad prism version 8 was used for statistical analysis. Shapiro-Wilk normality test ($\alpha=0.05$) was performed. Non-parametric Mann-Whitney two tailed tests, parametric unpaired two-tailed t-tests, ordinary one-way ANOVA or Kruskal-Wallis tests were used. *P 0.05; **P 0.01; ***P 0.001; ****P 0.0001. Only statistically significant results are reported in the figures. Correlation analysis used the Spearman two-tailed non-parametric test.

Supplementary Material

Refer to Web version on PubMed Central for supplementary material.

Authors

Ilaria Esposito^{#1,§}, **Paola Cicconi**^{#2}, **Anna Morena D'Alise**^{#3,‡}, **Anthony Brown**¹, **Marialuisa Esposito**³, **Leo Swadling**^{1,†}, **Peter Johannes Holst**^{4,8,12}, **Maria Rosaria Bassi**⁴, **Mariano Stornaiuolo**⁵, **Federica Mori**³, **Ventzislav Vassilev**⁶, **Wenqin Li**¹, **Timothy Donnison**¹, **Chiara Gentile**⁷, **Bethany Turner**¹, **Annette von Delft**¹, **Mariarosaria Del Sorbo**³, **Federica Barra**³, **Alessandra Maria Contino**³, **Adele Abbate**³, **Ettore Novellino**⁵, **Allan Randrup Thomsen**⁸, **Jan Pravsgaard Christensen**⁸, **Armin Lahm**³, **Fabiana Grazioli**³, **Virginia Ammendola**³, **Loredana Siani**³, **Stefano Colloca**³, **Paul Klenerman**^{1,2}, **Alfredo**

Nicosia^{7,9,10}, Lucy Dorrell^{1,11}, Antonella Folgori^{3,*}, Stefania Capone^{3,*}, Eleanor Barnes^{1,2,*;‡}, on behalf of the PEACHI Consortium

The PEACHI Consortium: In addition to PEACHI Consortium members who are authors

Eleanor Barnes, Anthony Brown, Stefania Capone, Paola Cicconi, Lucy Dorrell, Ilaria Esposito, Marialuisa Esposito, Antonella Folgori, Federica Mori, Leo Swadling, Bethany Turner, Ventzislav Vassilev, Annette von Delft

the following PEACHI Consortium members are collaborators who have contributed to study design, data analysis and interpretation:

Carly Bliss¹, Emma Ghaffari¹, Felicity Hartnel¹¹, Jakub Kopycinski¹, Shokouh Makvandi-Nejad¹, Verity Nevin¹, Dorota Borys⁶, Dominique Boutriau⁶, Landry Cochard⁶, Lan Lin⁶, Frank Struyf⁶, Tomáš Hanke^{11,13}, Ciaran Bannan¹⁴, Colim Bergin¹⁴, Matthias Hoffman¹⁵, Patrick Schmid¹⁵, Pietro Vernazza¹⁵, Clair Gardiner¹⁶, Elena Woods¹⁶

The PEACHI Consortium: In addition to PEACHI Consortium members who are authors

Eleanor Barnes, Anthony Brown, Stefania Capone, Paola Cicconi, Lucy Dorrell, Ilaria Esposito, Marialuisa Esposito, Antonella Folgori, Federica Mori, Leo Swadling, Bethany Turner, Ventzislav Vassilev, Annette von Delft

Eleanor Barnes, Anthony Brown, Stefania Capone, Paola Cicconi, Lucy Dorrell, Ilaria Esposito, Marialuisa Esposito, Antonella Folgori, Federica Mori, Leo Swadling, Bethany Turner, Ventzislav Vassilev, Annette von Delft

the following PEACHI Consortium members are collaborators who have contributed to study design, data analysis and interpretation:

Carly Bliss¹, Emma Ghaffari¹, Felicity Hartnel¹¹, Jakub Kopycinski¹, Shokouh Makvandi-Nejad¹, Verity Nevin¹, Dorota Borys⁶, Dominique Boutriau⁶, Landry Cochard⁶, Lan Lin⁶, Frank Struyf⁶, Tomáš Hanke^{11,13}, Ciaran Bannan¹⁴, Colim Bergin¹⁴, Matthias Hoffman¹⁵, Patrick Schmid¹⁵, Pietro Vernazza¹⁵, Clair Gardiner¹⁶, Elena Woods¹⁶

Carly Bliss¹, Emma Ghaffari¹, Felicity Hartnel¹¹, Jakub Kopycinski¹, Shokouh Makvandi-Nejad¹, Verity Nevin¹, Dorota Borys⁶, Dominique Boutriau⁶, Landry Cochard⁶, Lan Lin⁶, Frank Struyf⁶, Tomáš Hanke^{11,13}, Ciaran Bannan¹⁴, Colim Bergin¹⁴, Matthias Hoffman¹⁵, Patrick Schmid¹⁵, Pietro Vernazza¹⁵, Clair Gardiner¹⁶, Elena Woods¹⁶

Affiliations

¹Nuffield Department of Medicine, University of Oxford, OX3 7BN Oxford, U.K ²The Jenner Institute Laboratories, Nuffield Department of Medicine, University of Oxford, OX3 7DQ Oxford, U.K ³ReiThera s.r.l., 00128 Rome, Italy ⁴Center for Medical Parasitology, University of Copenhagen, DK-2200 Copenhagen, Denmark ⁵Department of Pharmacy, University of Naples Federico II, 80131 Naples, Italy ⁶GSK Vaccines, 1330 Rixensart, Belgium ⁷Department of Molecular Medicine and Medical Biotechnology, University of Naples Federico II, 80131 Naples, Italy ⁸Department of Immunology and Microbiology, University of Copenhagen, DK-2200

Copenhagen, Denmark ⁹CEINGE-Biotecnologie Avanzate, via Gaetano Salvatore 486, 80145 Naples, Italy ¹⁰Keires AG, 4051 Basel, Switzerland ¹¹Oxford NIHR Biomedical Research Centre, OX3 9DU Headington, U.K ¹²InProTher ApS, BiInnovation Institute, 2200 Copenhagen, Denmark ¹³International Research Centre for Medical Sciences, Kumamoto University, 2-39-1 Kurokami Chuo-ku Kumamoto 860-855, Japan ¹⁴St James' Hospital, D08 NHY1, Dublin, Ireland ¹⁵Division of Infectious Diseases and Hospital Epidemiology, Kantonsspital St Gallen, 9007 St Gallen, Switzerland ¹⁶School of Biochemistry and Immunology, Trinity College, 152-160 Pearse Street, Dublin, Ireland

Acknowledgments

The authors are grateful for the assistance of Ian Poulton, Meg Baker, Celia Mitton, Natalie Lella, Jack Quaddy (Centre for Clinical Vaccinology and Tropical Medicine, University of Oxford), GSK for the support, especially Lan Lin and the volunteers for their participation.

The authors are indebted to the NIH tetramer core facility (Atlanta, US) for provision of MHC peptide complexes and to BEI Resources (Virginia, US) for provision of peptide panels.

The authors thank the Data Safety Monitoring Committee (DSCM) members Brian Angus (University of Oxford), Andri Rauch (University of Bern) and Heiner Wedemeyer (University Clinic Essen) for their guidance.

The authors are grateful to Professor Riccardo Cortese for his remarkable support and guide.

Funding

This work was supported by funding from the European Union Seventh Framework Programme (FP7/2007-2013) under the grant agreement for PEACHI (number 305632). Additional funding was received by GlaxoSmithKline (GSK). The study was also supported in part by UK National Institute for Health Research (NIHR) infrastructure through the NIHR Oxford Biomedical Research Centre and the NIH U19 AI082630. EB is/was funded by the Medical Research Council UK (MR/K010239/1), the Oxford NIHR Biomedical Research Centre and is an NIHR Senior Investigator. P.K. is funded by the Wellcome Trust (WT109965MA) and is an NIHR Senior Investigator. L.S. was funded by the Medical Research Council UK following the award of a CASE studentship (1890672).

The views expressed in this article are those of the author and not necessarily those of the NHS, the NIHR, or the Department of Health. E.B., L.D. and P.K. are Jenner Investigators.

Data and materials availability

All data associated with this study are present in the paper or Supplementary Materials. Human adenovirus vectors with mouse Ii fragments fused to OVA are available from GSK and Reithera with a material transfer agreement.

References

1. Schroder B. The multifaceted roles of the invariant chain CD74--More than just a chaperone. *Biochim Biophys Acta*. 2016; 1863:1269–1281. [PubMed: 27033518]
2. Holst PJ, Sorensen MR, Mandrup Jensen CM, Orskov C, Thomsen AR, Christensen JP. MHC class II-associated invariant chain linkage of antigen dramatically improves cell-mediated immunity induced by adenovirus vaccines. *J Immunol*. 2008; 180:3339–3346. [PubMed: 18292559]
3. Mikkelsen M, Holst PJ, Bukh J, Thomsen AR, Christensen JP. Enhanced and sustained CD8+ T cell responses with an adenoviral vector-based hepatitis C virus vaccine encoding NS3 linked to the MHC class II chaperone protein invariant chain. *J Immunol*. 2011; 186:2355–2364. [PubMed: 21257961]

4. Grujic M, Holst PJ, Christensen JP, Thomsen AR. Fusion of a viral antigen to invariant chain leads to augmented T-cell immunity and improved protection in gene-gun DNA-vaccinated mice. *J Gen Virol.* 2009; 90:414–422. [PubMed: 19141451]
5. Rowe HM, Lopes L, Ikeda Y, Bailey R, Barde I, Zenke M, Chain BM, Collins MK. Immunization with a lentiviral vector stimulates both CD4 and CD8 T cell responses to an ovalbumin transgene. *Molecular therapy : the journal of the American Society of Gene Therapy.* 2006; 13:310–319. [PubMed: 16275163]
6. Colloca S, Barnes E, Folgori A, Ammendola V, Capone S, Cirillo A, Siani L, Naddeo M, Grazioli F, Esposito ML, Ambrosio M, et al. Vaccine Vectors Derived from a Large Collection of Simian Adenoviruses Induce Potent Cellular Immunity Across Multiple Species. *Science Translational Medicine.* 2012; 4
7. Spencer AJ, Cottingham MG, Jenks JA, Longley RJ, Capone S, Colloca S, Folgori A, Cortese R, Nicosia A, Bregu M, Hill AV. Enhanced vaccine-induced CD8+ T cell responses to malaria antigen ME-TRAP by fusion to MHC class II invariant chain. *PLoS One.* 2014; 9 e100538 [PubMed: 24945248]
8. Capone S, Naddeo M, D'Alise AM, Abbate A, Grazioli F, DelGaudio A, DelSorbo M, Esposito ML, Ammendola V, Perretta G, Taglioni A, et al. Fusion of HCV nonstructural antigen to MHC class II-associated invariant chain enhances T-cell responses induced by vectored vaccines in nonhuman primates. *Mol Ther.* 2014; 22:1039–1047. [PubMed: 24476798]
9. Halbroth BR, Sebastian S, Poyntz HC, Bregu M, Cottingham MG, Hill AVS, Spencer AJ. Development of a Molecular Adjuvant to Enhance Antigen-Specific CD8(+) T Cell Responses. *Sci Rep.* 2018; 8 15020 [PubMed: 30301933]
10. Jensen S, Steffensen MA, Jensen BA, Schluter D, Christensen JP, Thomsen AR. Adenovirus-based vaccine against *Listeria monocytogenes*: extending the concept of invariant chain linkage. *J Immunol.* 2013; 191:4152–4164. [PubMed: 24043891]
11. Sorensen MR, Holst PJ, Pircher H, Christensen JP, Thomsen AR. Vaccination with an adenoviral vector encoding the tumor antigen directly linked to invariant chain induces potent CD4+ T-cell-independent CD8+ T-cell-mediated tumor control. *European journal of immunology.* 2009; 39:2725–2736. [PubMed: 19637230]
12. Barnes E, Folgori A, Capone S, Swadling L, Aston S, Kurioka A, Meyer J, Huddart R, Smith K, Townsend R, Brown A, et al. Novel adenovirus-based vaccines induce broad and sustained T cell responses to HCV in man. *Sci Transl Med.* 2012; 4 115ra111
13. Colloca S, Barnes E, Folgori A, Ammendola V, Capone S, Cirillo A, Siani L, Naddeo M, Grazioli F, Esposito ML, Ambrosio M, et al. Vaccine vectors derived from a large collection of simian adenoviruses induce potent cellular immunity across multiple species. *Sci Transl Med.* 2012; 4 115ra112
14. Hayton EJ, Rose A, Ibrahimsa U, Del Sorbo M, Capone S, Crook A, Black AP, Dorrell L, Hanke T. Safety and tolerability of conserved region vaccines vectored by plasmid DNA, simian adenovirus and modified vaccinia virus ankara administered to human immunodeficiency virus type 1-uninfected adults in a randomized, single-blind phase I trial. *PLoS One.* 2014; 9 e101591 [PubMed: 25007091]
15. Swadling L, Capone S, Antrobus RD, Brown A, Richardson R, Newell EW, Halliday J, Kelly C, Bowen D, Fergusson J, Kurioka A, et al. A human vaccine strategy based on chimpanzee adenoviral and MVA vectors that primes, boosts, and sustains functional HCV-specific T cell memory. *Science Translational Medicine.* 2014; 6 261ra153
16. Hill AV, Reyes-Sandoval A, O'Hara G, Ewer K, Lawrie A, Goodman A, Nicosia A, Folgori A, Colloca S, Cortese R, Gilbert SC, et al. Prime-boost vectored malaria vaccines: progress and prospects. *Hum Vaccin.* 2010; 6:78–83. [PubMed: 20061802]
17. Antrobus RD, Coughlan L, Berthoud TK, Dicks MD, Hill AV, Lambe T, Gilbert SC. Clinical assessment of a novel recombinant simian adenovirus ChAdOx1 as a vectored vaccine expressing conserved Influenza A antigens. *Mol Ther.* 2014; 22:668–674. [PubMed: 24374965]
18. ManjalyThomas ZR, Satti I, Marshall JL, Harris SA, Lopez Ramon R, Hamidi A, Minhinick A, Riste M, Stockdale L, Lawrie AM, Vermaak S, et al. Alternate aerosol and systemic immunisation with a recombinant viral vector for tuberculosis, MVA85A: A phase I randomised controlled trial. *PLoS Med.* 2019; 16 e1002790 [PubMed: 31039172]

19. Weber J, Mandala M, Del Vecchio M, Gogas HJ, Arance AM, Cowey CL, Dalle S, Schenker M, Chiarion-Sileni V, Marquez-Rodas I, Grob JJ, et al. Adjuvant Nivolumab versus Ipilimumab in Resected Stage III or IV Melanoma. *N Engl J Med.* 2017; 377:1824–1835. [PubMed: 28891423]
20. Cappuccini F, Pollock E, Stribbling S, Hill AVS, Redchenko I. 5T4 oncofoetal glycoprotein: an old target for a novel prostate cancer immunotherapy. *Oncotarget.* 2017; 8:47474–47489. [PubMed: 28537896]
21. Organisation WH. WHO global hepatitis report. 2017.
22. Hill AM, Nath S, Simmons B. The road to elimination of hepatitis C: analysis of cures versus new infections in 91 countries. *J Virus Erad.* 2017; 3:117–123. [PubMed: 28758018]
23. Hahn JA, Wylie D, Dill J, Sanchez MS, Lloyd-Smith JO, Page-Shafer K, Getz WM. Potential impact of vaccination on the hepatitis C virus epidemic in injection drug users. *Epidemics.* 2009; 1:47–57. [PubMed: 20445816]
24. Scott N, McBryde E, Vickerman P, Martin NK, Stone J, Drummer H, Hellard M. The role of a hepatitis C virus vaccine: modelling the benefits alongside direct-acting antiviral treatments. *BMC Med.* 2015; 13:198. [PubMed: 26289050]
25. Stone J, Martin NK, Hickman M, Hellard M, Scott N, McBryde E, Drummer H, Vickerman P. The Potential Impact of a Hepatitis C Vaccine for People Who Inject Drugs: Is a Vaccine Needed in the Age of Direct-Acting Antivirals? *PLoS One.* 2016; 11 e0156213 [PubMed: 27224423]
26. Lauer GM, Barnes E, Lucas M, Timm J, Ouchi K, Kim AY, Day CL, Robbins GK, Casson DR, Reiser M, Dusheiko G, et al. High resolution analysis of cellular immune responses in resolved and persistent hepatitis C virus infection. *Gastroenterology.* 2004; 127:924–936. [PubMed: 15362047]
27. Fitzmaurice K, Petrovic D, Ramamurthy N, Simmons R, Merani S, Gaudieri S, Sims S, Dempsey E, Freitas E, Lea S, McKiernan S, et al. Molecular footprints reveal the impact of the protective HLA-A*03 allele in hepatitis C virus infection. *Gut.* 2011
28. Kim AY, Kuntzen T, Timm J, Nolan BE, Baca MA, Reyor LL, Berical AC, Feller AJ, Johnson KL, Schulze zur Wiesch J, Robbins GK, et al. Spontaneous control of HCV is associated with expression of HLA-B 57 and preservation of targeted epitopes. *Gastroenterology.* 2011; 140:686–696. e681 [PubMed: 20875418]
29. Grakoui A, Shoukry NH, Woollard DJ, Han J-H, Hanson HL, Ghayeb J, Murthy KK, Rice CM, Walker CM. HCV persistence and immune evasion in the absence of memory T cell help. *Science.* 2003; 302:659–662. [PubMed: 14576438]
30. Folgori A, Capone S, Ruggeri L, Meola A, Sporeno E, Ercole BB, Pezzanera M, Tafi R, Arcuri M, Fattori E, Lahm A, et al. A T-cell HCV vaccine eliciting effective immunity against heterologous virus challenge in chimpanzees. *Nature medicine.* 2006; 12:190–197.
31. Capone S, Naddeo M, D'Alise AM, Abbate A, Grazioli F, Del Gaudio A, Del Sorbo M, Esposito ML, Ammendola V, Perretta G, Taglioni A, et al. Fusion of HCV Nonstructural Antigen to MHC Class II-associated Invariant Chain Enhances T-cell Responses Induced by Vectored Vaccines in Nonhuman Primates. *Molecular Therapy.* 2014
32. Hartnell F, Brown A, Capone S, Kopycinski J, Bliss C, Makvandi-Nejad S, Swadling L, Ghaffari E, Cicconi P, Del Sorbo M, Sbrocchi R, et al. A Novel Vaccine Strategy Employing Serologically Different Chimpanzee Adenoviral Vectors for the Prevention of HIV-1 and HCV Coinfection. *Front Immunol.* 2018; 9 3175 [PubMed: 30713538]
33. Baerlecken NT, Nothdorft S, Stummvoll GH, Sieper J, Rudwaleit M, Reuter S, Matthias T, Schmidt RE, Witte T. Autoantibodies against CD74 in spondyloarthritis. *Ann Rheum Dis.* 2014; 73:1211–1214. [PubMed: 23687263]
34. Baraliakos X, Baerlecken N, Witte T, Heldmann F, Braun J. High prevalence of anti-CD74 antibodies specific for the HLA class II-associated invariant chain peptide (CLIP) in patients with axial spondyloarthritis. *Ann Rheum Dis.* 2014; 73:1079–1082. [PubMed: 23644552]
35. de Winter JJ, van de Sande MG, Baerlecken N, Berg I, Ramonda R, van der Heijde D, van Gaalen FA, Witte T, Baeten DL. Anti-CD74 antibodies have no diagnostic value in early axial spondyloarthritis: data from the spondyloarthritis caught early (SPACE) cohort. *Arthritis Res Ther.* 2018; 20:38. [PubMed: 29490705]

36. Gerlach JT, Ulsenheimer A, Gruner NH, Jung MC, Schraut W, Schirren CA, Heeg M, Scholz S, Witter K, Zahn R, Vogler A, et al. Minimal T-cell-stimulatory sequences and spectrum of HLA restriction of immunodominant CD4+ T-cell epitopes within hepatitis C virus NS3 and NS4 proteins. *J Virol.* 2005; 79:12425–12433. [PubMed: 16160170]
37. Schulze zur Wiesch J, Ciuffreda D, Lewis-Ximenez L, Kasprovicz V, Nolan BE, Streck H, Aneja J, Reyor LL, Allen TM, Lohse AW, McGovern B, et al. Broadly directed virus-specific CD4+ T cell responses are primed during acute hepatitis C infection, but rapidly disappear from human blood with viral persistence. *Journal of Experimental Medicine.* 2012; 209:61–75.
38. Schulze zur Wiesch J, Lauer GM, Day CL, Kim AY, Ouchi K, Duncan JE, Wurcel AG, Timm J, Jones AM, Mothe B, Allen TM, et al. Broad repertoire of the CD4+ Th cell response in spontaneously controlled hepatitis C virus infection includes dominant and highly promiscuous epitopes. *J Immunol.* 2005; 175:3603–3613. [PubMed: 16148104]
39. Northfield JW, Loo CP, Barbour JD, Spotts G, Hecht FM, Klenerman P, Nixon DF, Michaëlsson J. Human Immunodeficiency Virus Type 1 (HIV-1)-Specific CD8+ TEMRA Cells in Early Infection Are Linked to Control of HIV-1 Viremia and Predict the Subsequent Viral Load Set Point. 2007 *Journal of...*
40. Sridhar S, Begom S, Bermingham A, Hoschler K, Adamson W, Carman W, Bean T, Barclay W, Deeks JJ, Lalvani A. Cellular immune correlates of protection against symptomatic pandemic influenza. *Nature Publishing Group.* 2013; 19:1305–1312.
41. Reyes-Sandoval A, Wyllie DH, Bauza K, Milicic A, Forbes EK, Rollier CS, Hill AVS. CD8+ T effector memory cells protect against liver-stage malaria. *The Journal of Immunology.* 2011; 187:1347–1357. [PubMed: 21715686]
42. Brewerton DA, Hart FD, Nicholls A, Caffrey M, James DC, Sturrock RD. Ankylosing spondylitis and HL-A 27. *Lancet.* 1973; 1:904–907. [PubMed: 4123836]
43. Messina JP, Humphreys I, Flaxman A, Brown A, Cooke GS, Pybus OG, Barnes E. Global distribution and prevalence of hepatitis C virus genotypes. *Hepatology.* 2014
44. Capone S, Meola A, Ercole BB, Vitelli A, Pezzanera M, Ruggeri L, Davies M-E, Tafi R, Santini C, Luzzago A, Fu T-M, et al. A novel adenovirus type 6 (Ad6)-based hepatitis C virus vector that overcomes preexisting anti-ad5 immunity and induces potent and broad cellular immune responses in rhesus macaques. *Journal of virology.* 2006; 80:1688–1699. [PubMed: 16439526]
45. Roederer M, Nozzi JL, Nason MC. SPICE: Exploration and analysis of post-cytometric complex multivariate datasets. *Cytometry Part A.* 2011; 79A:167–174.
46. Shankar G, Devanarayan V, Amaravadi L, Barrett YC, Bowsher R, Finco-Kent D, Fiscella M, Gorovits B, Kirschner S, Moxness M, Parish T, et al. Recommendations for the validation of immunoassays used for detection of host antibodies against biotechnology products. *J Pharm Biomed Anal.* 2008; 48:1267–1281. [PubMed: 18993008]
47. Holst PJ, Christensen JP, Thomsen AR. Vaccination against lymphocytic choriomeningitis virus infection in MHC class II-deficient mice. *J Immunol.* 2011; 186:3997–4007. [PubMed: 21357263]
48. Aste-Amézaga M, Bett AJ, Wang F, Casimiro DR, Antonello JM, Patel DK, Dell EC, Franlin LL, Dougherty NM, Bennett PS, Perry HC, et al. Quantitative adenovirus neutralization assays based on the secreted alkaline phosphatase reporter gene: application in epidemiologic studies and in the design of adenovectors vaccines. *Human gene therapy.* 2004; 15:293–304. [PubMed: 15018738]

One Sentence Summary

Administration of an MHC-II invariant chain-adjuvanted HCV vaccine in humans leads to enhanced immunogenicity via the proteasome pathway.

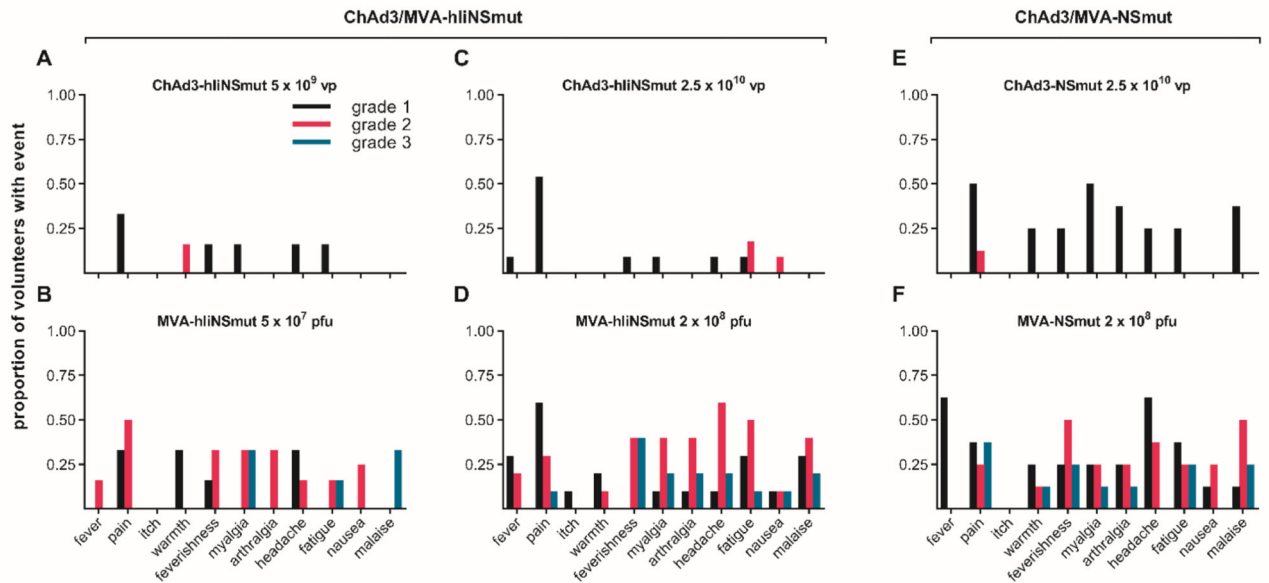


Figure 1. Solicited adverse events within 7 days from vaccination

Frequency of local and systemic adverse events recorded by volunteers on diary cards. The proportion of volunteers reporting symptoms at any time during 72 hours following (A) Low dose: ChAd3-hiNSmut (5×10^9 vp) (n=6); (B) Low dose: MVA-hiNSmut (5×10^7 pfu) (n=6), (C) Standard dose: ChAd3-hiNSmut (2.5×10^{10} vp) (n=11); (D) Standard dose: MVA-hiNSmut (2×10^8 pfu) (n=10); (E) Standard dose: ChAd3-NSmut (2.5×10^{10} vp) and (F) Standard dose: MVA-NSmut (2×10^8 pfu). Color code indicates maximum severity of the reaction reported: black– Grade 1 (mild); red– Grade 2 (moderate); blue–Grade 3 (severe).

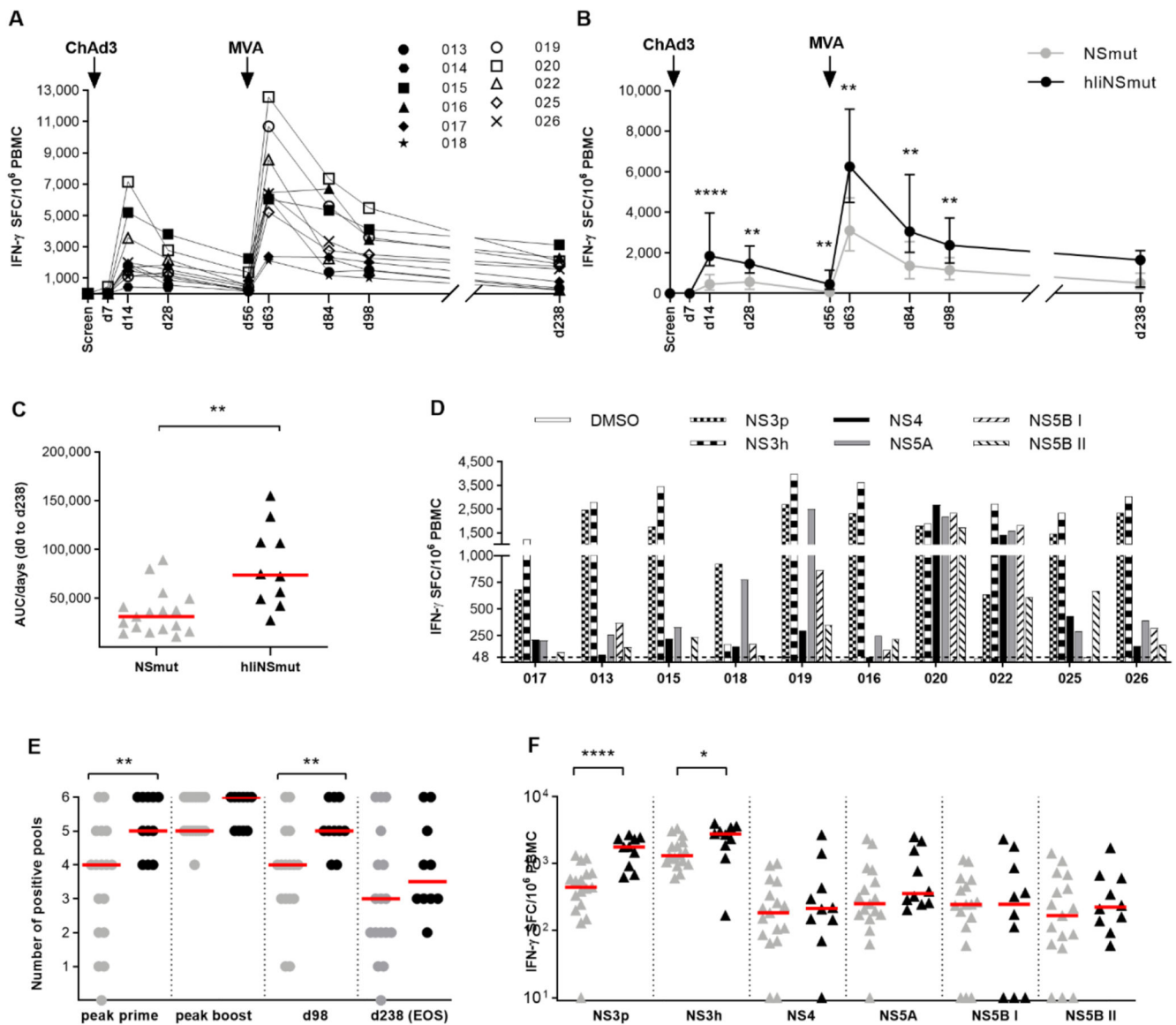


Figure 2. Kinetics and breadth of T cell response to hliNS after prime/boost vaccine regimen. (A) The kinetics of ex vivo IFN- γ ELISpot response to the NS region of HCV is shown for 10 volunteers who received ChAd3/MVA-hliNSmut vaccination and 1 volunteer (014) who received only ChAd3-hliNSmut over time calculated by summing the responses of positive pools corrected for background. (B) Comparisons of IFN- γ ELISpot response to HCV NS in volunteers receiving ChAd3/MVA-hliNSmut (black; n=10) or ChAd3/MVA-NSmut (grey; n=17). The median and IQR is shown. Arrows above graph indicate vaccination timepoints. (Two-tailed Mann-Whitney test at d14, d28, d56, d63, d84, d98) (C) Area Under the Curve (AUC) analysis up to d238 timepoint for total IFN- γ ELISpot response (Two-tailed Mann-Whitney test). Bars represent median. (D) Magnitude of T cell response to each NS region at d63. (E) The number of positive peptide pools for each volunteer is shown at peak post prime (d14 or d28), peak post boost (d63 or d84), d98 and EOS. (Two-tailed Mann-Whitney test post prime and at d98). Bars represent median. (F) Magnitude of T cell response to six

peptide pools at D63, 1-week post MVA vaccination (Two-tailed Mann-Whitney test for NS3p and NS3h). Bars represent median. Only statistically significant differences are shown. *P 0.05; **P 0.01; ****P 0.0001

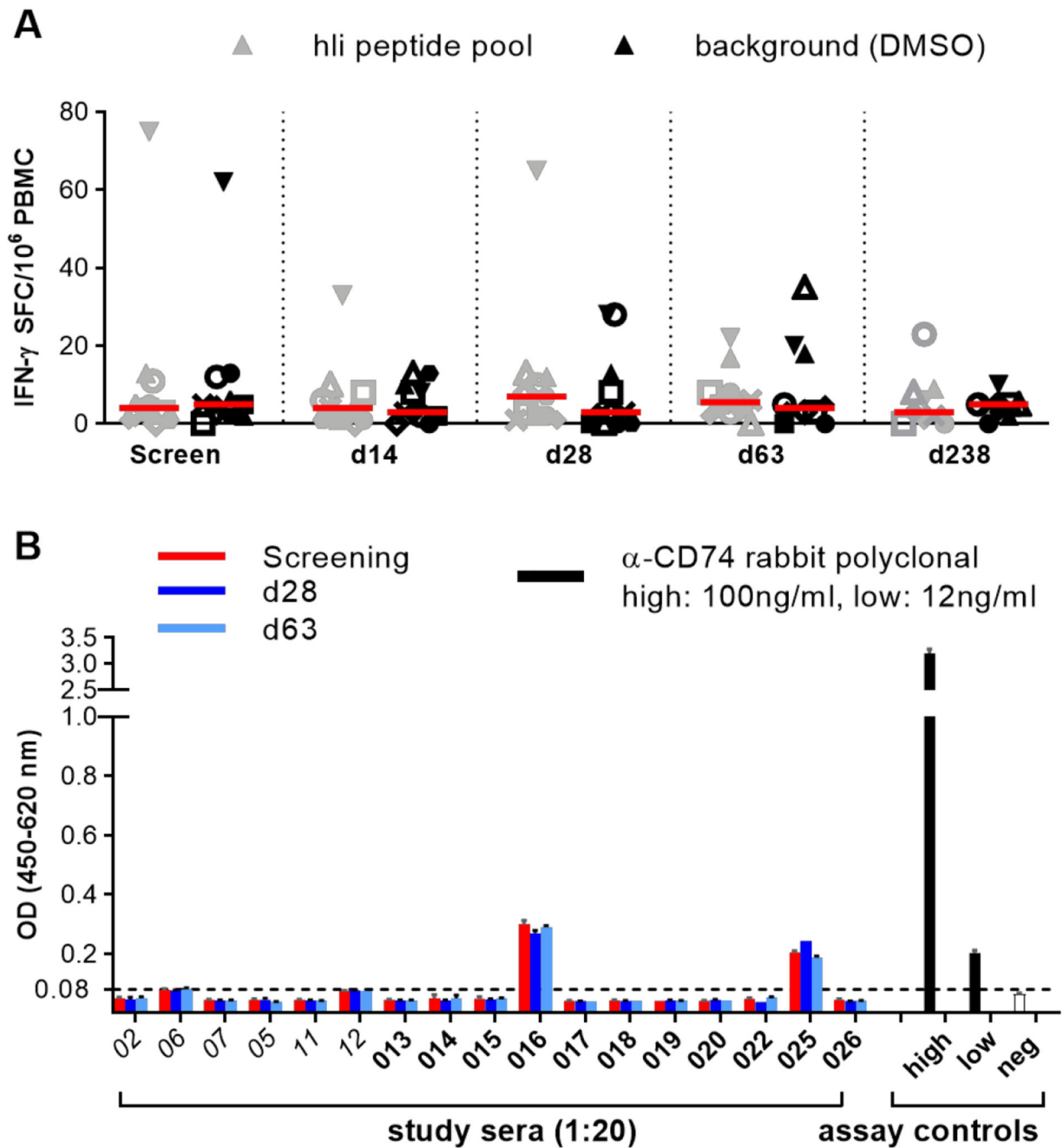


Figure 3. T cell and antibody response against Ii.

(A) IFN- γ ELISpot response against human Ii peptide pool at different time points: screening, d14, d28, (n= 11) and d63 and d238 (n= 10) for volunteers in group 2. Bars represent median. Each symbol represents T cell response to Ii in a specific subject at different time points of the prime/boost regimen.

(B) Antibody response to human CD74 p35 ectodomain in sera from individual volunteers collected at key time-points (screen, d28, d63) as detected by ELISA (n=17). Italics denotes group 1 volunteers, bars represent the mean absorbance (OD, optical density) of triplicate

wells plus standard deviation of 1:20 diluted sera or assay positive and negative controls. The dotted line set at 0.08 OD represents the assay positivity cut point, calculated as described in materials and methods.

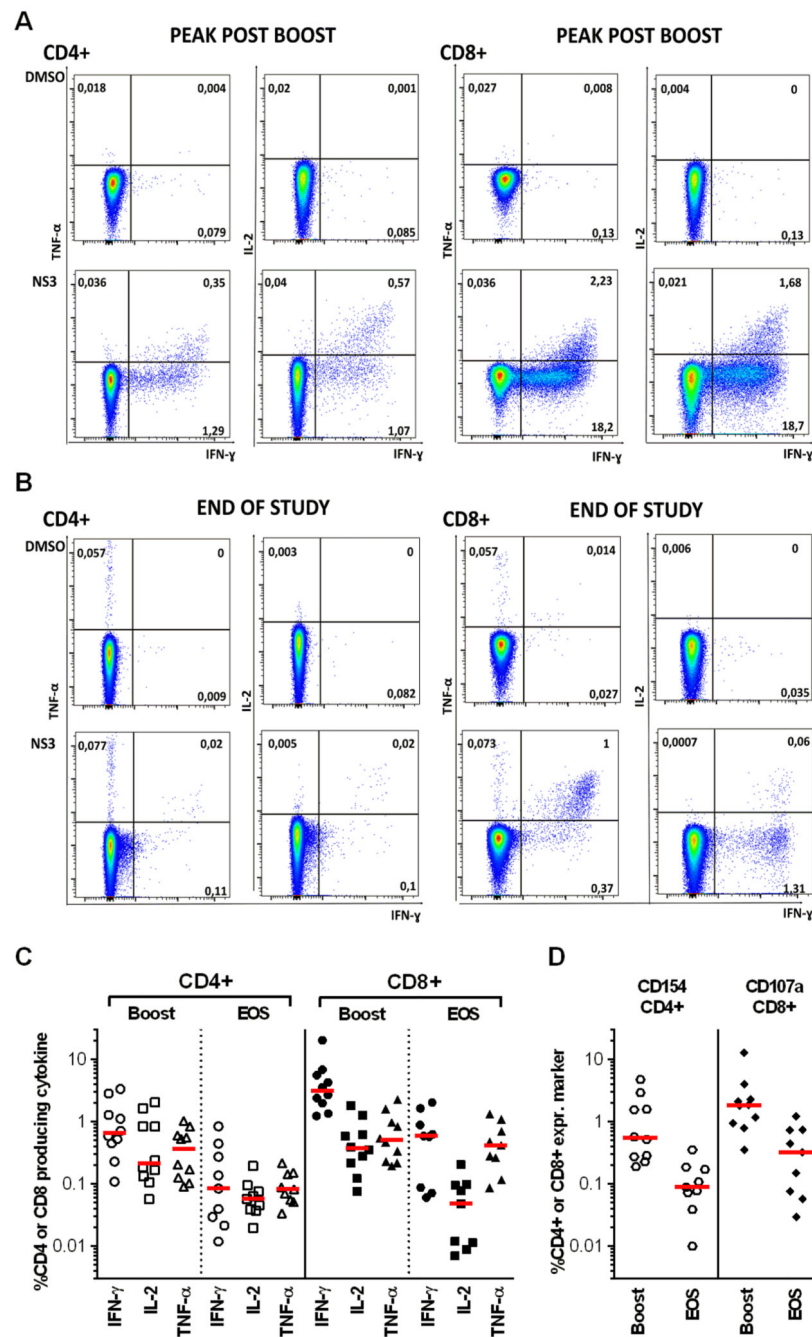


Figure 4. Functionality of vaccine-induced CD4+ and CD8+ T cells

(A-B) Example FACS plots showing TNF- α /IFN- γ and IL-2/IFN- γ after ICS of CD4+ and CD8+ T cells stimulated with DMSO as negative control and NS3-4 peptide pool one week after MVA-hIiNSmut boost vaccination (A) and at the end of study (EOS) (B). (C) Percentage of total CD4+ and CD8+ T cells producing IFN- γ , IL-2 or TNF- α after stimulation with NS3-5 peptide pools is shown at peak post-boost vaccination (n=10) and at EOS (n=9). Bars represent the median. (D) Percentage of CD4+ expressing CD154 and CD8+ expressing CD107a at peak post-boost and EOS.

CD8+ expressing CD107a after stimulation with NS3-5 peptide pools at peak post-boost (n=10) and at EOS (n=9). Bars represent the median.

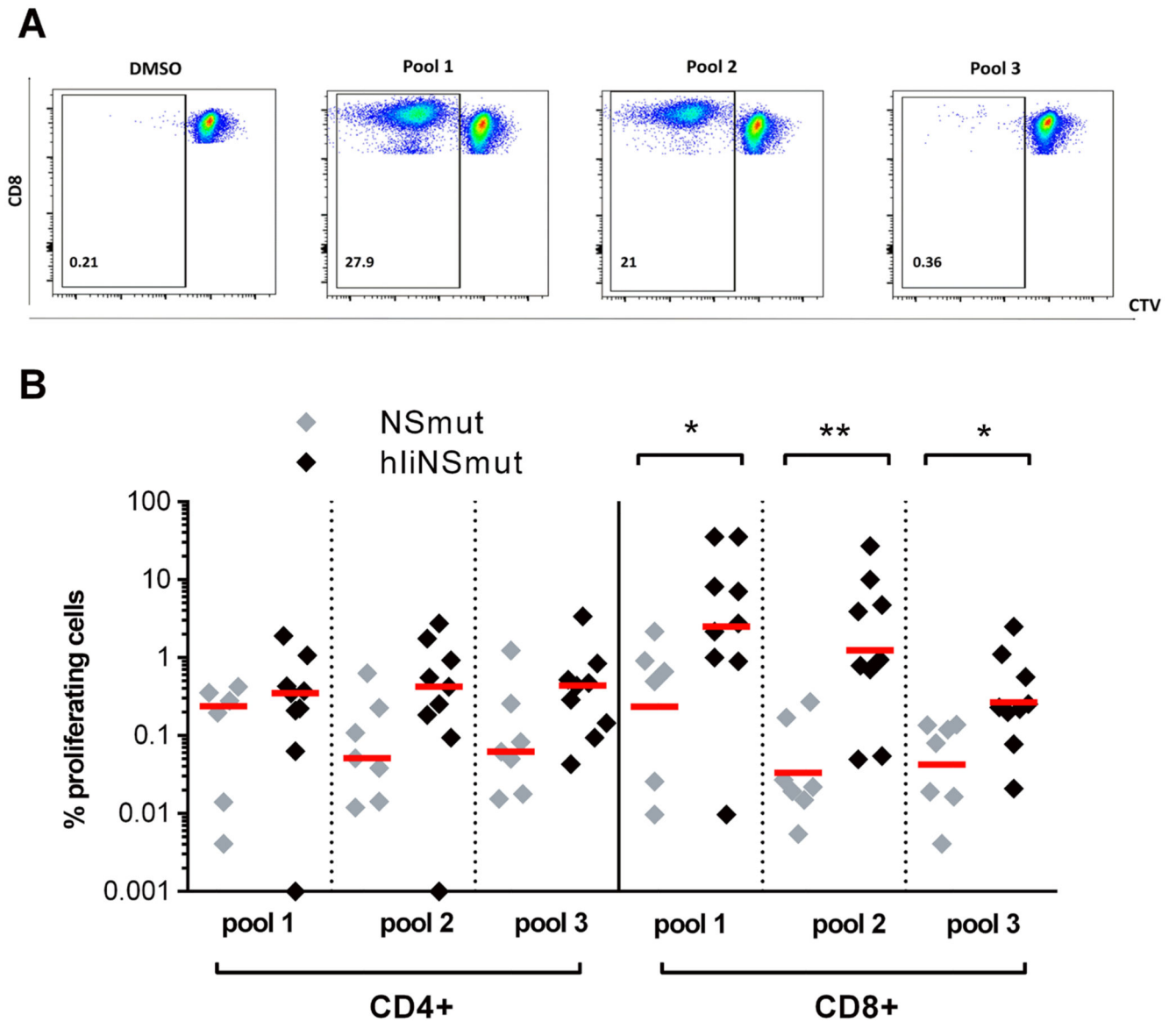


Figure 5. Sustained and enhanced proliferative T cell capacity after ChAd3/MVA-hIiNS vaccination regimen.

(A) Example FACS plots of proliferated CD8⁺ T cells after stimulation with pool 1 (first highest pool at boost), pool 2 (second highest pool at boost) and pool 3 (lowest at EOS but positive at boost) using cell trace violet reagent in T cell proliferation assays.

(B) Percentage of proliferated CD4⁺ and CD8⁺ T cells of subjects vaccinated with ChAd3/MVA-NSmut (grey, n=7) and ChAd3/MVA-hIiNSmut (black, n=9) at EOS after stimulation with peptide pools (Two-tailed Mann-Whitney test for CD8⁺ pool 1, pool 2 and pool 3).

Only statistically significant differences are shown. Bars represent median. *P 0.05; **P 0.01;

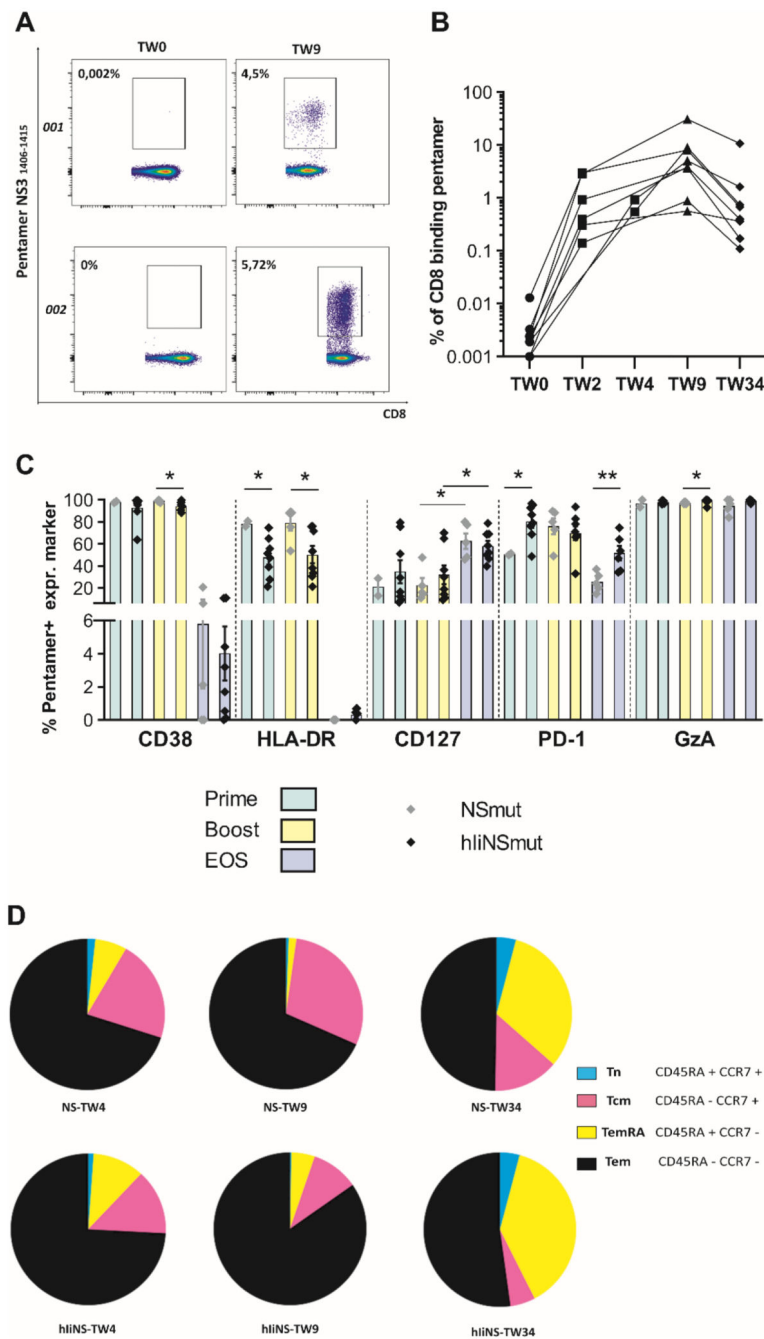


Figure 6. Phenotyping of pentamer+ CD8+ HCV-specific vaccine-induced T cells

(A) Example FACS plots of ex vivo staining of PBMC with using MHC class I pentamer A2-HCV NS3 1406-1415 in volunteers 001 (vaccinated with ChAd3/MVA-NSmut) and 002 (vaccinated with ChAd3/MVA-hIiNSmut) at baseline (TW0) and at peak post-boost (TW9). Values indicate percentage of CD8+ T cells binding pentamer. (B) The percentage of CD8+ T cells binding pentamer (HLA-A1-HCV 1435-1443 and HLA-A2-HCV 1406-1415) is shown over time for individual volunteers receiving ChAd3- /MVA-hIiNSmut vaccination (based on the peak of IFN- γ ELISpot response, % of pent+CD8+ are shown at TW2 or

TW4). Based on HLA, a single pentamer is used for each volunteer. (C) The percentage of the pentamer+ cells expressing phenotypic markers CD38, HLA-DR, CD127, PD-1 and Granzyme A (GzA) of volunteers vaccinated with ChAd3/MVA-NSmut (gray symbols) or ChAd3/MVA-hiNSmut (black symbols) at peak post-prime (green bars; gray, n=2 and black, n=8), at peak post-boost (yellow bars; gray, n=5 and black, n=8) and at EOS (light blue bars; gray, n=5 and black, n=8). Only statistically significant differences are shown (Two-tailed Mann-Whitney test CD38; Two-tailed Mann-Whitney test HLA-DR at prime and boost; Two-tailed Unpaired Student's t test CD127 gray symbols boost vs EOS; black symbols boost vs EOS; Two-tailed Unpaired Student's t test PD-1 at prime and EOS; Two-tailed Mann-Whitney test GzA). Mean with SEM is shown. (D) Pie charts display the proportion of pentamer+ CD8+ Tn, TemRA, Tcm, and Tem subsets for the two vaccination regimens as specified by staining for CD45RA and CCR7 at peak post-prime (NSmut, n=2; hiNSmut n=8) at peak post-boost and EOS (NSmut, n=5; hiNSmut n=8). Pie base, Median. *P 0.05; **P 0.01

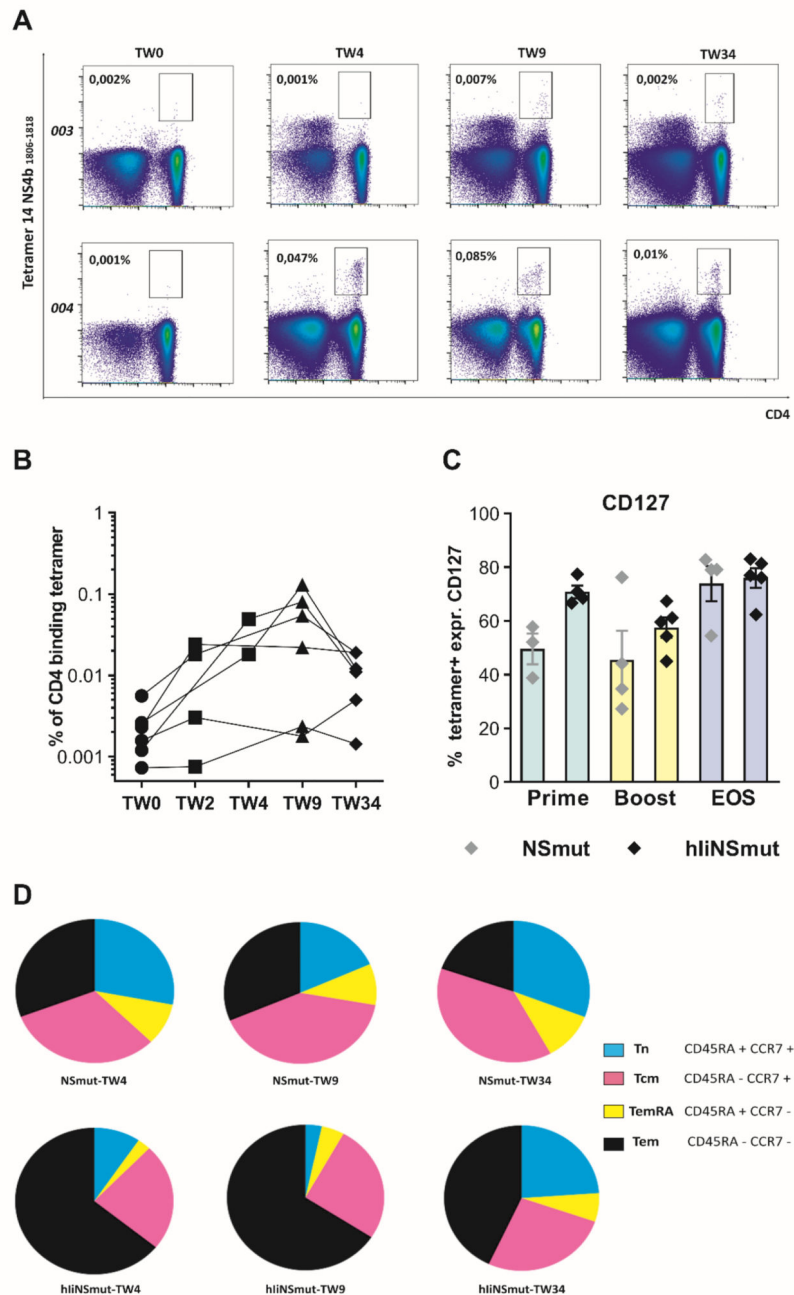


Figure 7. Phenotyping of tetramer+ CD4+ HCV-specific vaccine-induced T cells.

(A) Example FACS plots of ex vivo staining with MHC class II tetramer DRB01*01 NS31806-1818 in volunteers 003 (vaccinated with ChAd3/MVA-NSmut) and 004 (vaccinated with ChAd3/MVA-hiNSmut) over the study time course. (B) The percentage of specific CD4+ T cells stained with a single tetramer (for PEA03-01113,17, 18, 22) or a combination of them (for PEA03-01119, 26) is shown over time for individual volunteer receiving ChAd3-hiNSmut/MVA-hiNSmut vaccination (n=6). (C) The percentage of the tetramer+ cells expressing CD127 from volunteers vaccinated with ChAd3/MVA-NSmut

(grey symbols) or ChAd3/MVA-hIiNSmut (black symbols) at peak post-prime (green bars; grey n=3, black n=4), at peak post-boost (yellow bars; grey n=4, black n=5) and EOS (light blue bars; grey n=4, black n=5). Only statistically significant differences are shown. **(D)** Pie charts display the proportion of tetramer+ CD4 Tn, TemRA, Tcm, and Tem subsets over the course of the study for the two vaccination regimens, as specified by staining for CD45RA and CCR7 at peak post-prime (NSmut, n=3; hIiNSmut n=4) at peak post-boost and EOS (NSmut, n=4; hIiNSmut n=5). Pie base, Median.

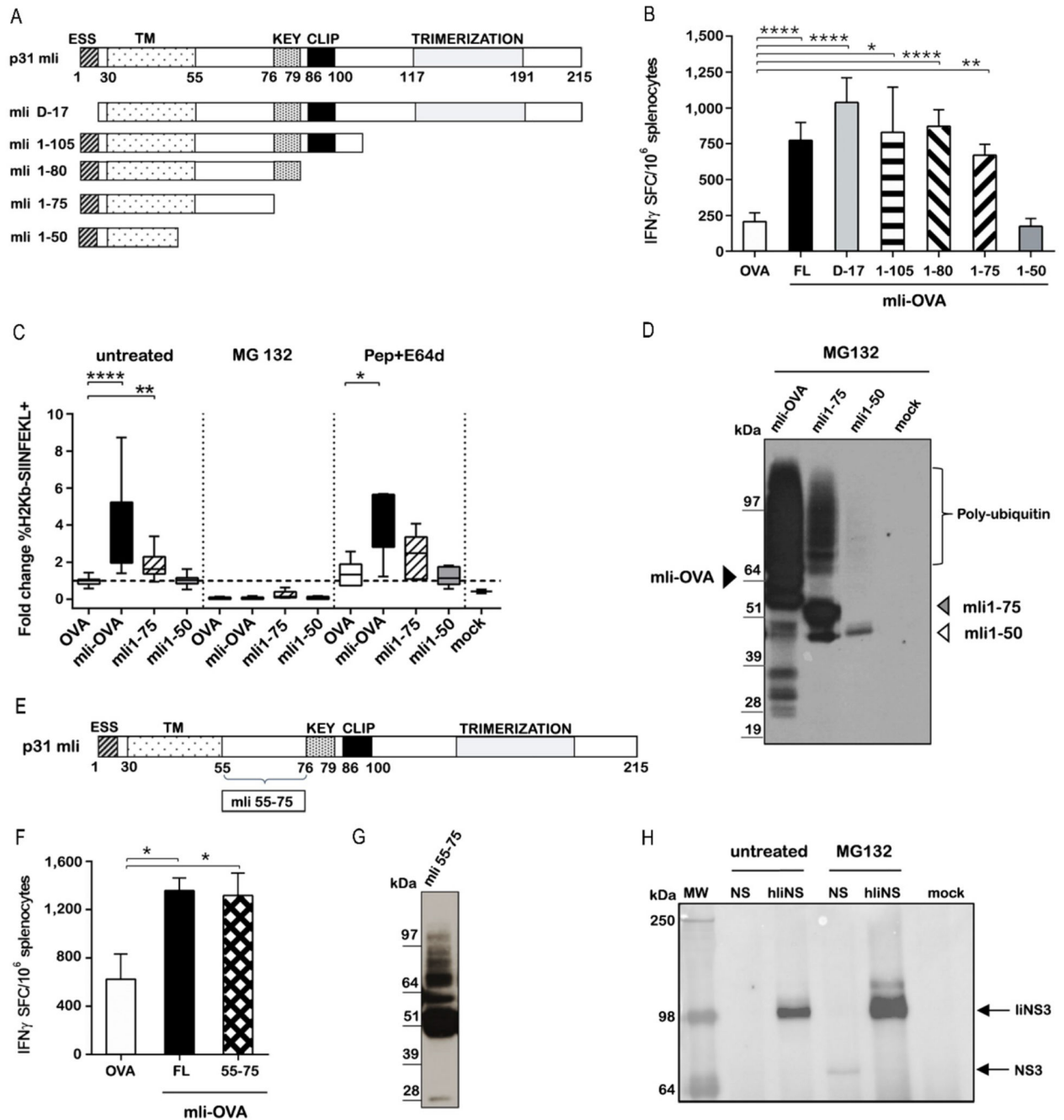


Figure 8. Ii modulates CD8⁺ T cell immune responses by targeting fused antigens for K48-specific ubiquitination and proteasome-mediated degradation.

(A) Schematic representation of full-length murine p31 Invariant chain (mLi) and deletion mutants. Functional domains are indicated: ESS, endolysosomal sorting signal; TM, transmembrane domain; KEY, key motif; CLIP, class II-associated Ii chain peptide; Trimerization, trimerization domain. (B) C57BL/6 mice were vaccinated with 3×10^6 viral particles of Ad5 encoding OVA either alone or fused to the indicated mLi deletion mutants. T cell responses were evaluated 2 weeks later by IFN- γ ELISpot assay. Data are expressed as

number of T cells producing IFN- γ per million splenocytes (Ordinary one-way ANOVA test for FL, D-17, 1-105, 1-80, 1-75 mLi constructs versus OVA) The experiment were repeated four times. **(C)** The percentage of Ad5 infected CD11c+ BMDC cells expressing SIINFEKL peptide bound to H-2Kb MHC class I left untreated or treated with MG132 (proteasome inhibitor) or Pepstatin A/E64 (lysosomal proteases inhibitor) was evaluated. Results are expressed as fold difference relative to Ad5-OVA infected cells (Kruskal-Wallis test untreated OVA vs mLi-OVA; OVA vs mLi1-75; Pepstatin+E64d treatment OVA vs mLi-OVA) The experiments were repeated five times in duplicate. **(D)** HeLa cells transiently transfected with ubiquitin plasmid were infected with Ad5-mLi-OVA, mLi1-75 OVA and mLi1-50 OVA and treated with MG132. Cells extracts were immunoprecipitated with anti-Lys48 antibody and analysed by WB with an anti-HA antibody detecting OVA. **(E)** Schematic representation of mLi and 55-75 region. **(F)** Immunogenicity in C57BL/6 mice of Ad5-mLi55-75 was evaluated after 2 weeks later by IFN- γ ELISpot assay (Ordinary one-way ANOVA mLi OVA versus OVA; mLi55-75 OVA versus OVA). The experiments were performed three times. **(G)** HeLa cells were transfected with ubiquitin plasmid, infected with Ad5 -mLi55-75 and treated with MG132. The cells lysate was immunoprecipitated using an anti-Lys48 antibody and tested by WB using anti HA antibody detecting OVA. The experiments were performed two times. **(H)** HeLa transiently transfected with ubiquitin plasmid were infected with ChAd3-NSmut and with ChAd3-hLiNSmut and treated or not with MG132. Cells extracts were immunoprecipitated with anti-Lys48 antibody and analysed by WB with an anti-NS3 Ab detecting NS3 protein. Mock is negative control for uninfected cells. The experiments were performed three times. *P 0.05; **P 0.01; ****P 0.0001